pieces of the BGVs turning sideways as previously we reported [15], we could have made a graft of a diameter of 1.1 cm and a length of 3.2 cm. This could be another option for making a longer or thicker graft.

The indication for reconstruction of the MHV might be controversial. We reconstructed the MHV in case 3 because (1) the patient had undergone preoperative chemotherapy and hepatic arterial infusion and might have potentially impaired hepatic function, and (2) we already had performed multiple partial resections of the liver and had to preserve the remnant hepatic function as far as possible. Recently, the necessity of reconstruction of the MHV has been advocated during living donor liver transplantation (LDLT) using right liver grafts [26–28]. Sano et al. [29] has demonstrated the indication for MHV reconstruction using the temporary artery occlusion test and Doppler ultrasonography. In review of the CT images, we can estimate that a cylindrical graft, 6 cm in length, could be prepared from the BGVs in almost all of the female patients and about two thirds of the male patients. Many types of venous graft have been used for the reconstruction of the MHV; the BGVs graft may be an option for reconstruction of the MHV during LDLT.

Conclusion

We presented successful three cases of major venous reconstruction using a cylindrical or patch graft customized from the BGVs. It is important to estimate the DR of the graft/the major replacing vein on preoperative CT scan and to plan the method of venous resection and reconstruction. A cylindrical graft made from the BGVs would be better utilized in female patients than in male patients.

Acknowledgments Supported in part by Grant-in-Aid for scientific research from the Ministry of Education, Science and Culture, and the Ministry of Health and Welfare of Japan

References

1. Fuhrman GM, Leach SD, Staley CA, Cusack JC, Charnsangavej C, Cleary KR, El-Naggar AK, Fenoglio CJ, Lee JE, Evans DB (1996) Rationale for en bloc vein resection in the treatment of pancreatic adenocarcinoma adherent to the superior mesenteric–portal vein confluence. Pancreatic Tumor Study Group. Ann Surg 223:154–162. doi:10.1097/00000658-199602000-00007
2. Evans DB, Lee JE, Leach SD, Fuhrman GM, Cusack JC Jr, Rich TA (1996) Vascular resection and intraoperative radiation therapy during pancreaticoduodenectomy: rationale and technique. Adv Surg 29:235–262
3. Harrison LE, Brennan MF (1997) Portal vein involvement in pancreatic cancer: a sign of unresectability? Adv Surg 31:375–394
4. Miyazaki M, Itoh H, Kaiho T, Ambiru S, Togawa A, Sasada K, Shiobara M, Shimizu Y, Yoshioka S, Yoshitome H, Nakajima N (1995) Portal vein reconstruction at the hepatic hilus using a left renal vein graft. J Am Coll Surg 180:497–498
5. Ohwada S, Hamada K, Kawate S, Sunose Y, Tomizawa N, Yamada T, Okabe T, Ogawa T, Sato Y (2007) Left renal vein graft for vascular reconstruction in abdominal malignancy. World J Surg 31:1215–1220. doi:10.1007/s00268-007-9015-5
6. Smoot RL, Christein JD, Farnell MB (2007) An innovative option for venous reconstruction after pancreaticoduodenectomy: the left renal vein. J Gastrointest Surg 11:425–431. doi:10.1007/s11605-007-0131-1
7. Choudry H, Avella D, Garcia L, Han D, Staveley-O'Carroll K, Kimchi E (2008) Use of the left renal vein as a practical conduit in superior mesenteric vein reconstruction. J Surg Res 146:117–120. doi:10.1016/j.jss.2007.07.022
8. Suzuki T, Yoshidome H, Kimura F, Shimizu H, Ohtsuka M, Kato A, Yoshitomi H, Nozawa S, Sawada S, Miyazaki M (2006) Renal function is well maintained after use of left renal vein graft for vascular reconstruction in hepatobiliary–pancreatic surgery. J Am Coll Surg 202:87–92. doi:10.1016/j.jamcollsurg.2005.08.001
9. Ohwada S, Takeyoshi I, Ogawa T, Ohya T, Saitoh A, Kawashima K, Iino Y, Morishita Y (1998) Hepatic vein reconstruction at inferior vena cava confluence using left renal vein graft. Hepatogastroenterology 45:1833–1836
10. Nakamura S, Sakaguchi S, Kitazawa T, Suzuki S, Koyano K, Muro H (1990) Hepatic vein reconstruction for preserving remnant liver function. Arch Surg 125:1455–1459
11. Nakamura S, Sakaguchi S, Hachiya T, Suzuki S, Nishiyama R, Konno H, Muro H, Baba S (1993) Significance of hepatic vein reconstruction in hepatectomy. Surgery 114:59–64
12. Kaneoka Y, Yamaguchi A, Isogai M, Hori A (2000) Hepatic vein reconstruction by external iliac vein graft using vascular clips. World J Surg 24:377–382. doi:10.1007/s002689910060
13. Allema JH, Reinders ME, van Gulik TM, van Leeuwen DJ, de Wit LT, Verbeek PC, Gouma DJ (1994) Portal vein resection in patients undergoing pancreatoduodenectomy for carcinoma of the pancreatic head. Br J Surg 81:1642–1649. doi:10.1002/bjs.1800811126
14. Nakamura S, Hachiya T, Oonuki Y, Sakaguchi S, Konno H, Baba S (1993) A new technique for avoiding difficulty during reconstruction of the superior mesenteric vein. Surg Gynecol Obstet 177:521–523
15. Sakamoto Y, Yamamoto J, Saiura A, Koga R, Kokudo N, Kosuge T, Yamaguchi T, Muto T, Makuuchi M (2004) Reconstruction of hepatic or portal veins by use of newly customized great saphenous vein grafts. Langenbecks Arch Surg 389:110–113. doi:10.1007/s00423-003-0452-9
16. Urayama H, Katada S, Matsumoto I, Ishida F, Ohmura K, Watanabe Y, Muroki T (1993) Reconstruction of jugular and portal blood flows using remodeled great saphenous vein grafts. Surg Today 23:936–938. doi:10.1007/BF00311377
17. Doty DB, Baker WH (1976) Bypass of superior vena cava with spiral vein graft. Ann Thorac Surg 22:490–493
18. Kubota K, Makuuchi M, Sugawara Y, Midorikawa Y, Sakamoto Y, Takayama T, Harihara Y (1998) Reconstruction of the hepatic and portal veins using a patch graft from the right ovarian vein. Am J Surg 176:295–297. doi:10.1016/S0002-9610(98)00149-4
19. Heavrin BS, Wrenn K (2007) Ovarian vein thrombosis: a rare cause of abdominal pain outside the peripartum period. J Emerg Med 34:67–69. doi:10.1016/j.jemermed.2007.05.034
20. Schwartz JH, Sclafani SJ, Glass TA, Sewell PE (2008) Acute gonadal vein thrombosis secondary to terminal ileitis and thrombophilia. J Urol 180:1124. doi:10.1016/j.juro.2008.06.075
21. Hiromura T, Nishioka T, Nishioka S, Ikeda H, Tomita K (2004) Reflux in the left ovarian vein: analysis of MDCT findings in asymptomatic women. AJR Am J Roentgenol 183:1411–1415
22. Rebner M, Gross BH, Korobkin M, Ruiz J (1989) Appearance of right gonadal vein. J Comput Assist Tomogr 13:460–462. doi:10.1097/00004728-198905000-00017

23. Gokan T, Kushihashi T, Nobusawa H, Hashimoto T, Matsui S, Kitanosono T, Munechika H (2001) CT demonstration of dilated gonadal vein as a portosystemic shunt of mesenteric varices. J Comput Assist Tomogr 25:798–801. doi:10.1097/00004728-200109000-00021
24. Cancarini GC, Pola A, Pezzotti G, Tardanico R, Cozzoli A, Cunico SC (2002) Recovery of renal function after right nephrectomy, cavectomy and left renal vein ligation. J Nephrol 15:186–190
25. Leach SD, Lee JE, Charnsangavej C, Cleary KR, Lowy AM, Fenoglio CJ, Pisters PW, Evans DB (1998) Survival following pancreaticoduodenectomy with resection of the superior mesenteric-portal vein confluence for adenocarcinoma of the pancreatic head. Br J Surg 85:611–617. doi:10.1046/j.1365-2168.1998.00641.x
26. Lee S, Park K, Hwang S, Lee Y, Choi D, Kim K, Koh K, Han S, Choi K, Hwang K, Makuuchi M, Sugawara Y, Min P (2001) Congestion of right liver graft in living donor liver transplantation. Transplantation 71:812–814. doi:10.1097/00007890-200103270-00021
27. Ghobrial RM, Hsieh CB, Lerner S, Winters S, Nissen N, Dawson S, Amersi F, Chen P, Farmer D, Yersiz H, Busuttil RW (2001) Technical challenges of hepatic venous outflow reconstruction in right lobe adult living donor liver transplantation. Liver Transpl 7:551–555. doi:10.1053/jlts.2001.24910
28. Kubota T, Togo S, Sekido H, Shizawa R, Takeda K, Morioka D, Tanaka K, Endo I, Tanaka K, Shimada H (2004) Indication for hepatic vein reconstruction in living donor liver transplantation of right liver grafts. Transplant Proc 36:2263–2266. doi:10.1016/j.transproceed.2004.06.035
29. Sano K, Makuuchi M, Miki K, Maema A, Sugawara Y, Imamura H, Matsunami H, Takayama T (2002) Evaluation of hepatic venous congestion: proposed indication criteria for hepatic vein reconstruction. Ann Surg 236:241–247. doi:10.1097/00000658-200208000-00013

Synuclein-γ Is Closely Involved in Perineural Invasion and Distant Metastasis in Mouse Models and Is a Novel Prognostic Factor in Pancreatic Cancer

Taizo Hibi,[1,2,3] Taisuke Mori,[1] Mariko Fukuma,[1] Ken Yamazaki,[1] Akinori Hashiguchi,[1] Taketo Yamada,[1] Minoru Tanabe,[2] Koichi Aiura,[2] Takao Kawakami,[4] Atsushi Ogiwara,[5] Tomoo Kosuge,[3] Masaki Kitajima,[2] Yuko Kitagawa,[2] and Michiie Sakamoto[1]

Abstract **Purpose:** Perineural invasion is associated with the high incidence of local recurrence and a dismal prognosis in pancreatic cancer. We previously reported a novel perineural invasion model and distinguished high– and low–perineural invasion groups in pancreatic cancer cell lines. This study aimed to elucidate the molecular mechanism of perineural invasion.

Experimental Design: To identify key biological markers involved in perineural invasion, differentially expressed molecules were investigated by proteomics and transcriptomics. Synuclein-γ emerged as the only up-regulated molecule in high–perineural invasion group by both analyses. The clinical significance and the biological property of synuclein-γ were examined in 62 resected cases of pancreatic cancer and mouse models.

Results: Synuclein-γ overexpression was observed in 38 (61%) cases and correlated with major invasive parameters, including perineural invasion and lymph node metastasis ($P < 0.05$). Multivariate analyses revealed synuclein-γ overexpression as the only independent predictor of diminished overall survival [hazard ratio, 3.4 (95% confidence interval, 1.51-7.51)] and the strongest negative indicator of disease-free survival [2.8 (1.26-6.02)]. In mouse perineural invasion and orthotopic transplantation models, stable synuclein-γ suppression by short hairpin RNA significantly reduced the incidence of perineural invasion ($P = 0.009$) and liver/lymph node metastasis ($P = 0.019$ and $P = 0.020$, respectively) compared with the control.

Conclusions: This is the first study to provide *in vivo* evidence that synuclein-γ is closely involved in perineural invasion/distant metastasis and is a significant prognostic factor in pancreatic cancer. Synuclein-γ may serve as a promising molecular target of early diagnosis and anticancer therapy.

Pancreatic ductal adenocarcinoma is currently the fourth leading cause of cancer-related death in Western countries (1). At the time of diagnosis, >80% of patients have locally advanced or metastatic disease and thus are not amenable for resection (2). Even in patients who underwent a histologically curative operation, long-term survival is rare, with the overall 5-year survival rates ranging from 10% to 25% (3, 4). Extensive local infiltration and early lymphatic and hematogenous spread likely contribute to the poor outcome of pancreatic cancer. Various criteria, such as tumor size, negative resection margins, histologic differentiation, lymph node metastasis, vascular involvement, and perineural invasion, have been proposed as prognostic indicators, but the results to date have been inconsistent (3–6). Of these, aggressive tumor extension into the perineural space even in the early stage of disease is a distinct mode of tumor spread in pancreatic cancer. High prevalence of local tumor recurrence even after curative resection is attributed to the residual tumor cells in the nerves of the remnant pancreas as well as the extrapancreatic nerve plexus that are undetected during the operation, leading to diminished survival. The striking incidence of perineural invasion in pancreatic cancer, ranging from 50% to 90%, underscores its importance (5, 6).

Recently, we established a mouse perineural invasion model and five human pancreatic cancer cell lines were divided into the high and the low–perineural invasion group (7). In the current study, proteomic analysis was used to compare protein expression profiles between these two groups to identify

Authors' Affiliations: Departments of [1]Pathology and [2]Surgery, Keio University School of Medicine; [3]Hepatobiliary and Pancreatic Surgery Division, National Cancer Center Hospital; [4]Clinical Proteome Center, Tokyo Medical University; and [5]Medical ProteoScope Co., Ltd., Tokyo, Japan

Received 11/11/08; revised 1/14/09; accepted 1/20/09; published OnlineFirst 4/7/09.

Grant support: The 21st Century Center of Excellence program and Cancer Research from the Ministry of Education, Science and Culture of Japan, and the 3rd Term Comprehensive 10-Year Strategy for Cancer Control from the Ministry of Health, Labor, and Welfare of Japan.

The costs of publication of this article were defrayed in part by the payment of page charges. This article must therefore be hereby marked *advertisement* in accordance with 18 U.S.C. Section 1734 solely to indicate this fact.

Note: Supplementary data for this article are available at Clinical Cancer Research Online (http://clincancerres.aacrjournals.org/).

Requests for reprints: Michiie Sakamoto, Department of Pathology, Keio University School of Medicine, 35 Shinanomachi, Shinjuku-ku, Tokyo 160-8582, Japan. Phone: 81-3-5363-3764; Fax: 81-3-3353-3290; E-mail: msakamot@sc.itc.keio.ac.jp.

doi:10.1158/1078-0432.CCR-08-2946

Translational Relevance

Aggressive tumor extension into the perineural space and adjacent lymph nodes even in the early stage of disease is a distinct mode of tumor spread in pancreatic cancer; however, its molecular mechanism remains unclear. This is the first study describing *in vivo* evidence that synuclein-γ is closely involved in perineural invasion/distant metastasis using mouse models and is a significant predictor of survival in resected cases of pancreatic cancer. Because 33% of patients with stage I disease in our series showed synuclein-γ overexpression, synuclein-γ may become an indicator for early diagnosis. To optimize the magnitude of pancreatic surgery, the extent of neural plexus resection and lymph node dissection may be determined according to the preoperative synuclein-γ status. Stratification of resected cases by synuclein-γ status is also worth considering to customize postoperative multidisciplinary approach. Synuclein-γ may well serve as a novel molecular target of anticancer therapy of this devastating disease.

differentially expressed proteins that may play a role in perineural invasion, reflecting the more aggressive tumor phenotype. Among the overexpressed proteins that emerged from quantitative proteomics, we selected synuclein-γ (SNCG) for further investigation because its corresponding mRNA was also up-regulated in the high-perineural invasion group (7). To clarify the clinical significance of SNCG expression in pancreatic cancer, the medical records of resected cases were retrospectively reviewed, focusing on the correlations with clinicopathologic factors as well as prognosis. The effect of stable SNCG suppression in the high-perineural invasion group was evaluated *in vivo* using mouse perineural invasion and orthotopic transplantation models.

Materials and Methods

Cell lines and laboratory animals. Five human pancreatic cancer cell lines, Capan-1, Capan-2, AsPC-1, Panc-1, and HPAF-II, were obtained from the American Type Culture Collection. Eight- to 12-wk-old, nonobese diabetes/severe combined immunodeficient mice were used. All studies were conducted in accordance with the U.S. Public Health Service Policy on Humane Care and Use of Laboratory Animals, NIH.

Perineural invasion model and orthotopic (pancreas) transplantation model in mice. The human pancreatic cancer cell lines were harvested from confluent cultures, washed twice with PBS, and resuspended in a serum-free RPMI 1640. For the perineural invasion model, mice were anesthetized, and 6 to 7 × 10^6 viable tumor cells in 100 μL of cell suspension were injected s.c. on the midline of their backs at two sites using an inoculator fitted with a 23-gauge needle. Six to 8 wks after injection, the tumor was resected with a 5-mm margin of the neighboring skin to examine the degree of perineural invasion to the mouse s.c. nerves (7).

For the orthotopic transplantation model, the mice were anesthetized and the distal pancreas exteriorized as described previously (8), and ~ 10^6 viable tumor cells in 10 μL of cell suspension were injected into the pancreas using an inoculator with a 27-gauge needle. The pancreas was relocated into the abdominal cavity, and the peritoneum and skin were closed with a surgical stapler. Five to 6 wks after injection, the mice were sacrificed, and the pancreas, stomach, duodenum, liver, lymph nodes, lungs, and other organs of suspected tumor involvement or metastasis were harvested.

Proteomic analysis. Tumor cells of the human pancreatic cancer cell lines were homogenized in PBS supplemented with a protease inhibitor cocktail (Roche Diagnosis) and fractionated by ultracentrifugation (52,000 × *g*; 4°C; 20 mins). The resulting pellet, containing plasma membranes from the cells, was solubilized in PBS containing 5% SDS with continuous ultrasonication. The resulting solution was taken as the insoluble fraction, whereas the supernatant from the ultracentrifugation, containing mainly cytosolic proteins, was taken as the soluble fraction. An aliquot (50 μg of protein) from each fraction was subjected to SDS-PAGE on a 12.5% polyacrylamide gel 1 mm thick. SDS-PAGE was carried out until the bromophenol blue marker passed the boundary between the stacking and separation gels so that almost all proteins were condensed in a small area between the gel boundary and the blue marker. This small gel area was then excised from the gel slab, and the gel slice, including proteins, was subjected to in-gel tryptic digestion (9).

The resulting small peptide mixture (1 μg) was analyzed using a liquid chromatography-tandem mass spectrometry (MS/MS) system in a fully automated manner (10, 11). A reversed-phase peptide separation was done on a C18 capillary column (Michrom Bioresources) at a flow rate of 1 μL/min. The liquid chromatography effluent was directly interfaced with an electrospray ionization source in a positive ion mode modified on a Finnigan LTQ linear ion trap mass spectrometer (Thermo Fisher Scientific; ref. 12). The electrospray ionization-MS/MS operation and continuous data acquisition of full MS scan and subsequent three MS/MS scans were carried out on an Xcalibur system controller (Thermo Fisher Scientific).

All full MS data were investigated using an i-OPAL differential liquid chromatography -MS data analysis system (i-OPAL algorithm; patent WO2004/090526 AI). Firstly, the signal intensity of the full MS scan was normalized so that the total signal intensity of each data became the same value. Several standard signals, derived either from the coanalyzed egg white lysozyme or from sample intrinsic common proteins, were selected as i-OPAL alignment markers. The i-OPAL alignment program was used to align the nonlinearly fluctuating liquid chromatography retention time axis of all liquid chromatography -MS data to finally generate a single combined liquid chromatography -MS data for the soluble fraction and the insoluble fraction, respectively. A *t* test was applied for each peak signal in the final combined liquid chromatography -MS data to select candidate marker signals whose intensity differed significantly within a cell type. Statistical analysis was done using Spotfire DecisionSite software package.

All MS/MS data were investigated using Mascot search program (Matrix Science;[6] ref. 13) against the *Homo sapiens* (human) subset of the Swiss-Prot and the RefSeq protein sequence databases. The database searches were done allowing for fixed modification of cysteine residue (*S*-carbamidomethylation, +57.0 Da) and variable modification of methionine residue (oxidation, +16.0 Da), peptide mass tolerance at ±2.0 Da, and product ion tolerance at ±0.8 *m/z* unit.

The proteomic analysis was done in duplicate for each cell line. An liquid chromatography -MS/MS measurement generated a single two-dimensional signal profile and >10,000 product ion spectra acquired by dissociation of peptide ions. To identify proteins involved in perineural invasion, we compared the signal profiles between the high- and low-perineural invasion cell line groups. We filtered all the peaks detected in the signal profiles according to the following conditions: (*a*) the liquid chromatography retention time between 5 and 75 mins, (*b*) the *m/z* value of ≤1,500, and (*c*) the *P* value of the Student's *t* test between the high-perineural invasion and the low-perineural invasion groups <0.001.

Patients and resected specimens. We reviewed the medical records of 67 consecutive patients who underwent resection with curative intent for invasive ductal pancreatic adenocarcinoma from 1995 through 2004 at Keio University Hospital, Tokyo, Japan. Five patients who suffered

[6] http://www.matrixscience.com

in-hospital death were excluded, and a total of 62 patients with available follow-up data comprised the subjects of this retrospective study. Two pathologists examined all resected specimens to confirm the histopathologic diagnosis of pancreatic adenocarcinoma according to the Japan Pancreas Society Classification (14). The tumor node metastasis system of the Unio Internationale Contra Cancrum (UICC) was used for staging (15). This study was conducted under the approval of the Ethics Committee of Keio University School of Medicine (approval 16-34-1).

The definition and the degree of perineural invasion were determined as described previously (7). Other pathologic factors are summarized in Table 1. Outcome measures included disease-free and overall survival. The diagnosis of tumor recurrence or metastasis was based on radiological findings. Survival time was calculated as the period from the date of surgery until death or the most recent clinic visit.

Immunologic analysis and quantitative reverse transcriptase-PCR. A goat anti-SNCG polyclonal antibody (Santa Cruz Biotechnology) was utilized. Immunohistochemical staining was evaluated by two independent observers who were not aware of the clinicopathologic data of the corresponding tumor in the surgical cases and the SNCG suppression status in the mouse models. Positive control samples were described previously (16). In the surgical specimens, peripheral nerves also served as an internal control. SNCG positive was defined as ≥10% staining of the tumor. Immunofluorescence, Western blotting, and quantitative reverse transcriptase-PCR analysis were described previously (7). In quantitative reverse transcriptase-PCR, the primer set was 5′-AACACTGTGGCCACCAAGAC-3′ (forward) and 5′-GATGGCCTCAAGTCCTCCTT-3′ (reverse), which corresponds to the coding region of the SNCG transcript.

Vector construction and retroviral infection. Vector construction and production of recombinant retroviruses were described previously (17, 18). To generate two short hairpin RNA (shRNA) expression vectors for SNCG, that is, pSI-CMSCVpuro-H1R-SNCGshRNA-A and pSI-CMSCVpuro-H1R-SNCGshRNA-B, the targeted sequences were 5′-TGGAGGAGGCGGAGAACAT-3′ and 5′-CCGAGAAGACCAAGGAGCA-3′, respectively. For the control (nontargeting sequence) shRNA expression vector, namely, pSI-CMSCVpuro-H1R-Control, the sequence was 5′-TAAGGCTATGAAGAGATAC-3′. Two stable SNCG-suppressed Capan-1 cells and the Control Capan-1 cells were designated sh-A, sh-B, and sh-Control, respectively.

Statistical analysis. Unless otherwise indicated, all data were determined from three independent experiments, with each of them done in triplicate. The data are expressed as mean values ± SD. The mRNA levels of SNCG in each cell line were compared by Student's *t* test (two tailed). The χ^2 test or Fisher's exact probability test were used when appropriate to determine the correlations between clinicopathologic variables and SNCG expression. Survival rates were calculated with the Kaplan-Meier method, and the log-rank test was applied to compare survival between different groups. Significant prognostic factors revealed by the log-rank tests were included in the multivariate analysis using the Cox proportional hazard model. Statistical significance was defined as $P < 0.05$. All statistical analyses were done using SPSS statistical software (SPSS, Inc.).

Table 1. Correlations between SNCG expression and histopathologic factors

Variables	SNCG expression, *n* (%)		*P*
	Negative, *n* = 24	Positive, *n* = 38	
Tumor size, mm			0.014
≤20	11 (46)	6 (16)	
>20	13 (54)	32 (84)	
Serosal invasion			0.081
Absent	22 (92)	28 (74)	
Present	2 (8)	10 (26)	
Retroperitoneal extension			0.84
Absent	12 (50)	18 (47)	
Present	12 (50)	20 (53)	
Portal vein involvement			0.97
Absent	14 (58)	22 (58)	
Present	10 (42)	16 (42)	
Lymph node metastasis			0.009
Negative	12 (50)	7 (18)	
Positive	12 (50)	31 (82)	
Resection status			0.15
R0	19 (79)	24 (63)	
R1	5 (21)	14 (37)	
UICC stage			0.009
IA/IB/IIA	12 (50)	7 (18)	
IIB/III/IV	12 (50)	31 (82)	
Histologic differentiation			0.069
Well	11 (46)	9 (24)	
Moderate, poor	13 (54)	29 (76)	
Lymphatic invasion			0.091
0-1	16 (67)	17 (45)	
2-3	8 (33)	21 (55)	
Vascular invasion			0.027
0-1	17 (71)	16 (42)	
2-3	7 (29)	22 (58)	
Perineural invasion			0.033
0-1	12 (50)	9 (24)	
2-3	12 (50)	29 (76)	

Results

Proteomic analysis. We obtained 214 peaks in which 171 were up-regulated and 43 were down-regulated. A two-way hierarchical clustering algorithm successfully distinguished between the high-perineural invasion and the low-perineural invasion groups (Fig. 1A). Peptide identifications to the product ion spectra were screened according to a Mascot scoring value as the ion score representing the significance of identification. The peptide identification of the highest ion score with >30 was adopted per peak. Of the 214 peaks, 211 were linked to specific peptide identification, whereas the remaining 3 peaks were given with no identification under the present conditions. Database entry names from Swiss-Prot[7] or RefSeq[8] as the source of the peptide identifications are shown in Fig. 1A.

SNCG expression in human pancreatic cancer cell lines. Among the proteins listed in Fig. 1A, SNCG was selected for further investigation because its corresponding RNA level also showed significant up-regulation in the previous microarray analysis comparing the high- and low-perineural invasion groups (7). Quantitative reverse transcriptase-PCR was used for total RNA samples isolated from five pancreatic cancer cell lines to analyze the SNCG mRNA levels. The relative expression level of SNCG was significantly higher in the high-perineural invasion group compared with the low-perineural invasion group ($P = 0.0001$; Fig. 1B). Protein overexpression of SNCG in Capan-1 and Capan-2 was subsequently confirmed by Western blotting (Fig. 1B).

The immunohistochemical properties of cell lines for SNCG were evaluated in the tumors of the mouse perineural invasion model. SNCG staining was strongly positive (>90% of all tumor

[7] http://br.expasy.org/sprot/
[8] http://www.ncbi.nlm.nih.gov/RefSeq/

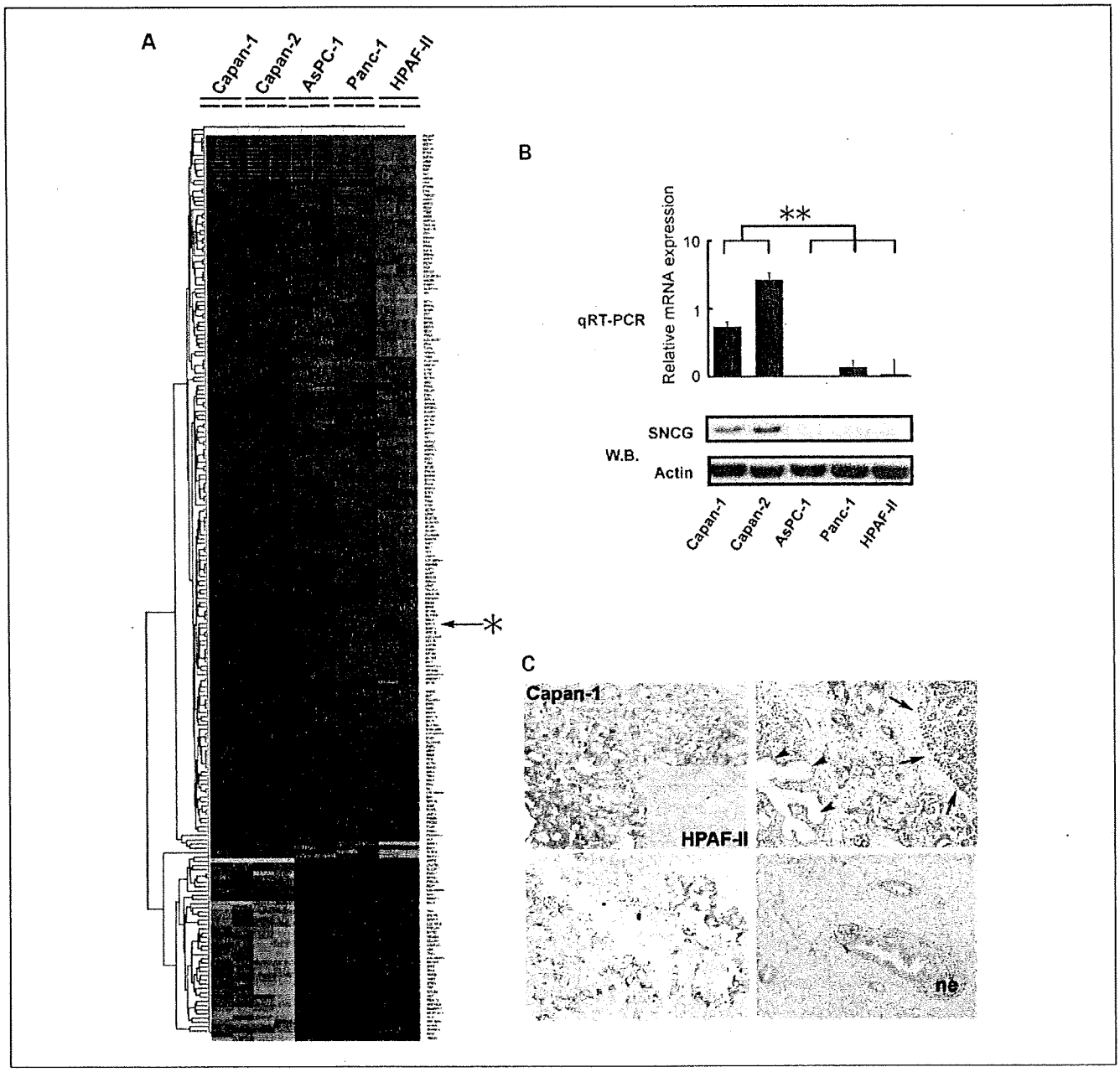

Fig. 1. *A*, proteomic analysis. Two-way hierarchical clustering algorithm successfully differentiated 214 peptide ion signals by peak intensity between high – perineural invasion (Capan-1 and Capan-2) and low – perineural invasion (AsPC-1, Panc-1, and HPAF-II) groups. Color patch, the peak intensity of the corresponding peptide in each cell line as a continuum of relative expression levels from lowest (*green*) to highest (*bright red*). *, SNCG. *B*, quantitative reverse transcriptase-PCR analysis and Western blotting. W.B., Western blotting. of SNCG in five human pancreatic cancer cell lines. SNCG mRNA and protein expression levels were significantly higher in the high – perineural invasion group compared with the low – perineural invasion group. **, $P = 0.0001$. *C, top left plate*, immunohistochemical properties of cell lines. Capan-1 showed strongly positive staining for SNCG compared with consistently negative HPAF-II (*inset*). *Top right/bottom left/bottom right plates*, in surgically resected specimens, the pancreatic cancer cells showed heterogeneous staining for SNCG, whereas the normal pancreas (*arrowheads*, pancreatic ducts; *arrows*, acinar cells) were mostly negative. ne, nerves.

cells) in the high – perineural invasion group, whereas the low – perineural invasion group was universally negative under the same condition (Fig. 1C). SNCG localization was observed mainly in the cytoplasm with focal nuclear staining.

Clinical significance of SNCG overexpression in resected cases of pancreatic cancer. The median age of the 62 patients (40 men and 22 women) meeting our eligibility criteria was 67 years (range, 45-83 years). Two tumors were categorized as UICC stage IA, 4 as stage IB, 13 as stage IIA, 34 as stage IIB, 1 as stage III, and 8 as stage IV. All stage IV cases were nodal metastasis beyond the regional lymph node station, including the para-aorta ($n = 6$), the distal mesenteric ($n = 1$), and the lesser curvature of the stomach ($n = 1$). Figure 1C exemplifies the representative SNCG staining properties of the resected specimens. The pancreatic ducts and the acinar cells of the nontumorous pancreas showed mostly negative to faint

staining. A wide range of immunoreactivity was observed in the surgical cases, varying from the cytoplasm only (focal or diffuse) to strong accumulation in the nuclei. The peripheral nerves constantly showed intense SNCG staining and therefore served as an internal positive control.

Of the total of 62 resected pancreatic cancer samples, 38 (61%) were positive and 22 (39%) were negative for SNCG staining. χ^2 analysis revealed that perineural invasion (grades 2 and 3) and other histologic markers of aggressive disease, including tumor size > 20 mm, positive lymph node metastasis, UICC stage > IIB, and vascular invasion (grades 2 and 3), were significantly associated with SNCG overexpression (Table 1).

During a median follow-up of 25 months (range, 4-171 months), the overall 5-year survival rate was 32%, with a median survival of 29 months [95% confidence interval (95% CI), 11-47 months]. Log-rank analysis showed that pancreatic cancer with SNCG overexpression had a significantly decreased overall survival, with a median of 15 months (95% CI, 9-22 months) compared with SNCG-negative tumors (median survival not reached; $P = 0.002$; Fig. 2). Positive lymph node metastasis, UICC stage ≥ IIB, moderately or poorly differentiated histology, and lymphatic invasion (grades 2 and 3) were also associated with a poor prognosis by univariate analysis (Table 2). Multivariate analysis based on the Cox proportional hazard model including these five factors revealed SNCG overexpression to be the only independent negative prognostic variable of overall survival (hazard ratio, 3.4; 95% CI, 1.51-7.51; $P = 0.003$). Meanwhile, patients having tumors with positive lymph node metastasis, UICC stage ≥ IIB, lymphatic/vascular invasion (grades 2 and 3), perineural invasion (grades 2 and 3), and SNCG overexpression were found to have significantly shorter disease-free survival (Table 2). By multivariate analysis, SNCG overexpression was the strongest negative predictor of disease-free survival (hazard ratio, 2.8; 95% CI, 1.26-6.02; $P = 0.011$), followed by positive lymph node metastasis (hazard ratio, 2.4; 95% CI, 1.03-5.57; $P = 0.044$).

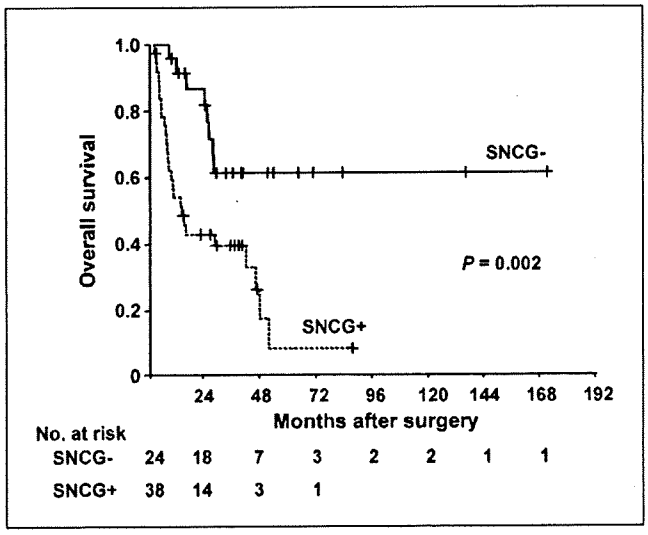

Fig. 2. Comparison of Kaplan-Meier survival curves. Patients with SNCG xoverexpression (*dotted line*) had a significantly poor prognosis compared with patients with negative SNCG expression (*solid line*).

Table 2. Log-rank univariate analysis of overall and disease-free survival

Variables	Overall survival		Disease-free survival	
	Median, mo	*P*	Median, mo	*P*
Tumor size, mm		0.059		0.060
≤20	NR		NR	
>20	25		13	
Serosal invasion		0.65		0.70
Absent	29		35	
Present	15		25	
Retroperitoneal extension		0.68		0.38
Absent	42		40	
Present	29		18	
Portal vein involvement		0.24		0.20
Absent	42		35	
Present	15		10	
Lymph node metastasis		0.016		0.006
Negative	NR		NR	
Positive	17		10	
Resection status		0.052		0.12
R0	42		35	
R1	12		8	
UICC stage		0.043		0.021
IA/IB/IIA	NR		NR	
IIB/III/IV	17		13	
Histologic differentiation		0.022		0.14
Well	NR		49	
Moderate, poor	25		18	
Lymphatic invasion		0.016		0.021
0-1	NR		40	
2-3	15		10	
Vascular invasion		0.23		0.030
0-1	42		NR	
2-3	18		13	
Perineural invasion		0.087		0.031
0-1	NR		NR	
2-3	26		12	
Intraoperative radiation		0.54		0.78
Yes	46		25	
No	28		28	
Adjuvant chemotherapy		0.14		0.98
Yes	42		18	
No	25		25	
SNCG expression		0.002		0.001
Negative	NR		NR	
Positive	15		10	

Abbreviation: NR, not reached.

Effect of SNCG suppression **in vitro** *and* **in vivo.** To determine whether SNCG is an instigator of invasion and metastasis or merely a correlative product during pancreatic cancer progression, the effect of SNCG suppression on high-perineural invasion group of human pancreatic cancer cell lines was further evaluated. Capan-1 was selected for the study because the infection rate of recombinant retroviruses with shRNA for SNCG was considerably lower in Capan-2 compared with Capan-1 (data not shown). Of the two stable SNCG-suppressed Capan-1 cells, a significant decrease of SNCG mRNA and protein levels in sh-A was shown by quantitative reverse transcriptase-PCR and Western blot analysis compared with sh-Control *in vitro* ($P < 0.0001$; Fig. 3A,). In sh-B, the decline was subtle and the difference was not statistically significant ($P = 0.096$; Fig. 3A).

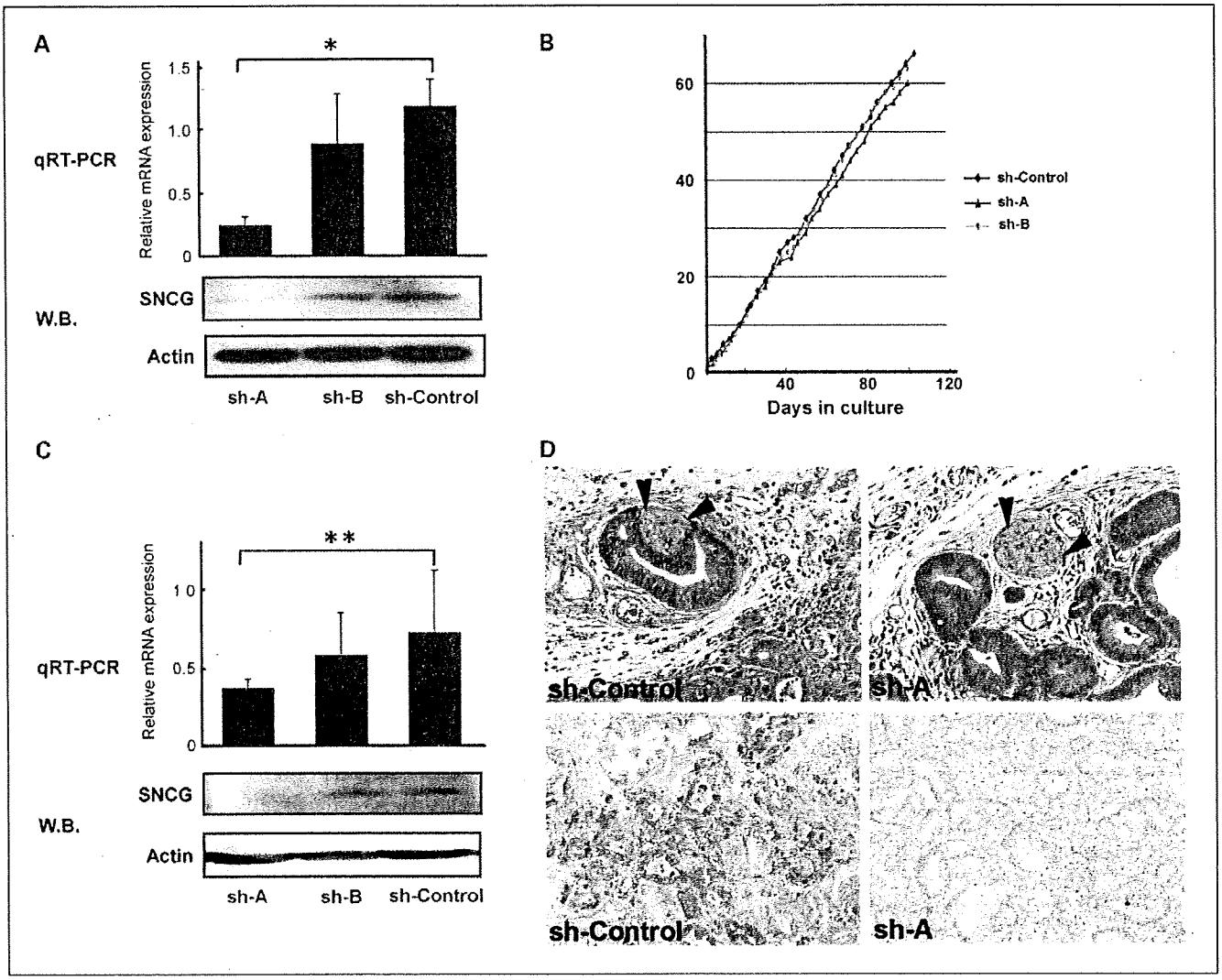

Fig. 3. *A*, quantitative reverse transcriptase-PCR analysis and Western blotting of SNCG in gene suppression study *in vitro* confirmed a substantial decrease in SNCG expression in sh-A compared with sh-Control. *, $P < 0.0001$. The difference was not statistically significant in sh-B ($P = 0.096$). *B, in vitro* growth curves of SNCG knockdown cells and control cells. The population doubling time of sh-A (*triangles*) was slightly extended compared with sh-Control (*diamonds*) and sh-B (*circles*). PD, population doubling time. *C*, quantitative reverse transcriptase-PCR and Western blotting of the s.c. tumors in mouse perineural invasion models revealed a stable *SNCG* gene knockdown effect in sh-A compared with sh-Control. **, $P = 0.018$. *D*, microscopic findings in mouse perineural invasion models. The tumor cells of sh-Control easily invaded the s.c. nerve (*arrowheads, top left plate*) and showed diffusely positive staining to SNCG (*bottom left plate*). In contrast, sh-A – derived tumors exhibited no perineural invasion, although the nerve (*arrowheads*) was involved within the tumor (i.e., nerve involvement, cancer nest includes nerves without direct contact between the tumor cells and the perineurium; *top right plate*). They were generally negative for SNCG (*bottom right plate*).

To determine whether SNCG suppression affects the *in vitro* growth of Capan-1 cells, cultures of sh-Control, sh-A, and sh-B were initially seeded at 1×10^5 cells/10-cm plate in 10 mL of RPMI 1640 serum. The population doubling time was roughly equivalent in the first 40 days in culture, although slight extension was observed in sh-A thereafter (Fig. 3B). Immunofluorescence analysis of sh-Control and sh-A under a confocal laser scanning microscope (LSM 510, Carl Zeiss) are shown in Supplementary Fig. S4A and B. In sh-Control, SNCG (*green*) diffusely localized to the cytoplasm, whereas in sh-A, the cytoplasmic SNCG signal was much lower, leaving only punctuate staining (Fig. 4A and B, respectively; Supplemental Data). No apparent difference was noted in cell shape and intercellular relations.

The results of mRNA assay and Western blotting of the s.c. tumors in the mouse perineural invasion model confirmed stable SNCG suppression in sh-A (Fig. 3C). In sh-B, the degree of down-regulation was mild, correlating with the *in vitro* results (Fig. 3A and C). In the mouse perineural invasion model, sh-A and -B showed significantly lower perineural invasion rates at 25% ($P = 0.009$) and 33% ($P = 0.026$), respectively, compared with the high perineural invasion incidence (82%) in sh-Control (Table 3). Tumor growth was also inhibited to some extent in the knockdown group, exhibiting a >25% size difference in sh-A ($P = 0.016$); however, the difference was not statistically significant in sh-B ($P = 0.27$; Table 3). A remarkable difference about the affinity of tumor cells to the mouse s.c. nerves was observed between sh-Control

and sh-A (Fig. 3D). The number of SNCG-positive cells was significantly smaller in sh-A (11% ± 11%; $P < 0.0001$) and sh-B (46% ± 12%; $P = 0.0005$) compared with sh-Control (65% ± 11%; Fig. 3D). In the invasive front of sh-Control–derived tumors, the cancer cells easily infiltrated into the muscle layers, whereas sh-A–derived tumors predominantly presented expansive growth (Supplementary Fig. S4C and D, respectively).

Because the clinicopathologic analysis of surgical cases suggest a strong correlation between SNCG overexpression and lymph node metastasis (Table 1), we constructed an orthotopic (pancreas) transplantation model to examine the SNCG knockdown effect on the metastatic potential of Capan-1 cells. In sh-A, the incidence of liver and lymph node metastasis remarkably decreased compared with sh-Control, developing in 0% (0 of 9; $P = 0.019$) and 22% (2 of 9; $P = 0.020$) of transplanted mice, respectively (Table 3). Although sh-B–derived tumors showed a mild reduction in the metastatic rate against sh-Control, the differences were not statistically significant (liver, $P = 0.28$; lymph node, $P = 0.51$). Representative microscopic findings of the liver and lymph node metastasis are shown in Supplementary Fig. S4E and F, respectively.

Discussion

This is the first study to provide *in vivo* evidence that SNCG is significantly correlated with perineural invasion as well as other major invasive parameters, including tumor size, vascular invasion, lymph node metastasis, and UICC stage, in patients with pancreatic cancer. The prognostic impact of SNCG overexpression was impressive; it was the only independent predictor of diminished overall survival and the strongest negative indicator of disease-free survival by multivariate analysis. Furthermore, SNCG gene silencing in mouse models of perineural invasion and orthotopic transplantation using human pancreatic cancer cell lines was associated with a dramatic reduction of perineural invasion as well as liver and lymph node metastasis, the main homing organs of pancreatic cancer cells. Our series shed light on the critical role of SNCG overexpression in acquiring invasive and metastatic properties.

SNCG has been shown to be involved in tumorigenesis and metastasis of a wide range of malignancies; nevertheless, only one report has documented SNCG overexpression in pancreatic cancer to date (16, 19–22). In breast cancer cell lines and mammary glands, chaperone-like activity of SNCG has been described (23, 24). SNCG may potentially exert various oncogenic roles in pancreatic cancer as a chaperone protein through stimulation of signal transduction pathways that regulate cell proliferation, invasion, and metastasis.

Zhu et al. (25) suggested that pancreatic cancer cells and nerves may interact in an autocrine/paracrine manner to provide microenvironment conducive for perineural invasion. Pancreatic cancers with overexpression of nerve growth factor in the cytoplasm of tumor cells and its high-affinity receptor, tyrosine kinase receptor A, in the perineurium of pancreatic nerves exhibited significantly higher perineural invasion rates and degree of pain. Meanwhile, in human pancreatic cancer cell lines, nerve growth factor–induced pancreatic cancer cell growth seems to be mediated by phosphorylation of tyrosine kinase receptor A and mitogen-activated protein kinase (26). Because SNCG overexpression was described to modulate mitogen-activated protein kinase pathways, leading to cell survival by inhibition of apoptotic activities (27), it may also promote nerve growth factor–tyrosine kinase receptor A signaling through its chaperone-like activity, contributing to perineural invasion in pancreatic cancer.

Previous studies have shown stage-specific SNCG up-regulation in advanced breast carcinomas and other malignancies, and our results are consistent with their observations (19–22). SNCG may be involved in pancreatic cancer progression by the induction of matrix metalloproteinases and its association in tumor cell-to-stroma interaction (28, 29). Meanwhile, SNCG was suggested to stimulate disassembly of neurofilament network and to interact with microtubule-associated proteins, thus influencing cytoskeletal integrity (30, 31). In our study, the mouse models apparently exhibited infiltrative and exaggerated growth of tumors with SNCG overexpression, although no obvious differences in cell proliferation or morphology were detected *in vitro* between cells overexpressing SNCG and knockdown cells. These findings indicate that SNCG overexpression may lead to a more malignant phenotype by altering the cell architecture, growth, and motility of pancreatic cancer cells as a chaperone protein in association with the tumor microenvironment.

Currently, proteomic analysis is emerging as a novel and powerful method of detecting proteins associated with pancreatic cancer progression (32, 33). We focused on the regulatory element of perineural invasion by comparing the proteomic profiles between high– and low–perineural invasion groups in human pancreatic cancer cell lines. Previously, proteomic

Table 3. Incidence of perineural invasion and tumor spread following s.c. injection and orthotopic transplantation of Capan-1: the impact of *SNCG* gene silencing by 2 different sequences

shRNAs	Perineural invasion model		Orthotopic transplantation model				
	Perineural invasion	Tumor size, mm	Ascites	Peritoneal dissemination	Distant metastasis		
					Liver	Lymph nodes	Lungs
sh-Control	9/11 (82%)	19 ± 5	7/7 (100%)	4/7 (57%)	4/7 (57%)	6/7 (86%)	0/7 (0%)
sh-A	3/12 (25%)*	14 ± 4†	4/9 (44%)†	1/9 (11%)	0/9 (0%)†	2/9 (22%)†	0/9 (0%)
sh-B	4/12 (33%)†	17 ± 4	7/7 (100%)	4/7 (57%)	2/7 (29%)	5/7 (71%)	0/7 (0%)

*$P < 0.01$ versus sh-Control.
†$P < 0.05$ versus sh-Control.

studies were used to differentiate protein expression profiles between pancreatic cancer tissues and normal or inflamed pancreas (32, 33), and our tumor phenotype-oriented approach may become a breakthrough to genetically tailored cancer diagnosis and therapy. In our series, 33% of patients with stage I disease showed SNCG overexpression. Several authors have detected SNCG in serum and urine samples of patients with malignant tumors (19, 20, 34) and SNCG as an indicator for early diagnosis warrants further investigation. Stratification of resected cases by SNCG status is worth considering to customize postoperative multidisciplinary approach.

In conclusion, this is the first report of *in vivo* evidence that SNCG overexpression is the key biological marker of increased malignant potential and is closely involved in perineural invasion and liver/lymph node metastasis in pancreatic cancer. In surgically resected cases, SNCG is a significant prognostic factor. SNCG may serve as a novel molecular target of early diagnosis as well as antimetastatic therapy.

Disclosure of Potential Conflicts of Interest

No potential conflicts of interest were disclosed.

Acknowledgments

We thank H. Suzuki, M. Morioka, and T. Iijima for their excellent technical support.

References

1. Jemal A, Siegel R, Ward E, Murray T, Xu J, Thun MJ. Cancer statistics, 2007. CA Cancer J Clin 2007;57:43–66.
2. Wray CJ, Ahmad SA, Matthews JB, Lowy AM. Surgery for pancreatic cancer: recent controversies and current practice. Gastroenterology 2005;128:1626–41.
3. Cleary SP, Gryfe R, Guindi M, et al. Prognostic factors in resected pancreatic adenocarcinoma: analysis of actual 5-year survivors. J Am Coll Surg 2004;198:722–31.
4. Sohn TA, Yeo CJ, Cameron JL, et al. Resected adenocarcinoma of the pancreas—616 patients: results, outcomes, and prognostic indicators. J Gastrointest Surg 2000;4:567–79.
5. Pour PM, Bell RH, Batra SK. Neural invasion in the staging of pancreatic cancer. Pancreas 2003;26:322–5.
6. Biankin AV, Morey AL, Lee CS, et al. DPC4/Smad4 expression and outcome in pancreatic ductal adenocarcinoma. J Clin Oncol 2002;20:4531–42.
7. Koide N, Yamada T, Shibata R, et al. Establishment of perineural invasion models and analysis of gene expression revealed an invariant chain (CD74) as a possible molecule involved in perineural invasion in pancreatic cancer. Clin Cancer Res 2006;12:2419–26.
8. Fu X, Guadagni F, Hoffman RM. A metastatic nude-mouse model of human pancreatic cancer constructed orthotopically with histologically intact patient specimens. Proc Natl Acad Sci U S A 1992;89:5645–9.
9. Shevchenko A, Wilm M, Vorm O, Mann M. Mass spectrometric sequencing of proteins from silver-stained polyacrylamide gels. Anal Chem 1996;68:850–8.
10. Maeda J, Hirano T, Ogiwara A, et al. Proteomic analysis of stage I primary lung adenocarcinoma aimed at individualisation of postoperative therapy. Br J Cancer 2008;98:596–603.
11. Kawakami T, Tateishi K, Yamano Y, Ishikawa T, Kuroki K, Nishimura T. Protein identification from product ion spectra of peptides validated by correlation between measured and predicted elution times in liquid chromatography/mass spectrometry. Proteomics 2005;5:856–64.
12. Schwartz JC, Senko MW, Syka JE. A two-dimensional quadrupole ion trap mass spectrometer. J Am Soc Mass Spectrom 2002;13:659–69.
13. Perkins DN, Pappin DJ, Creasy DM, Cottrell JS. Probability-based protein identification by searching sequence databases using mass spectrometry data. Electrophoresis 1999;20:3551–67.
14. Japan Pancreas Society. Classification of pancreatic carcinoma. 2nd English ed. Tokyo: Kanehara; 2003.
15. Sobin LH, Wittekind CH. TNM classification of malignant tumours. 6th ed. New York: Wiley-Liss; 2002. p. 93–6.
16. Li Z, Sclabas GM, Peng B, et al. Overexpression of synuclein-gamma in pancreatic adenocarcinoma. Cancer 2004;101:58–65.
17. Haga K, Ohno S, Yugawa T, et al. Efficient immortalization of primary human cells by $p16^{INK4a}$-specific short hairpin RNA or Bmi-1, combined with introduction of hTERT. Cancer Sci 2007;98:147–54.
18. Naviaux RK, Costanzi E, Haas M, Verma IM. The pCL vector system: rapid production of helper-free, high-titer, recombinant retroviruses. J Virol 1996;70:5701–5.
19. Liu H, Liu W, Wu Y, et al. Loss of epigenetic control of synuclein-gamma gene as a molecular indicator of metastasis in a wide range of human cancers. Cancer Res 2005;65:7635–43.
20. Jia T, Liu YE, Liu J, Shi YE. Stimulation of breast cancer invasion and metastasis by synuclein gamma. Cancer Res 1999;59:742–7.
21. Yanagawa N, Tamura G, Honda T, Endoh M, Nishizuka S, Motoyama T. Demethylation of the synuclein γ gene CpG island in primary gastric cancers and gastric cancer cell lines. Clin Cancer Res 2004;10:2447–51.
22. Wu K, Quan Z, Weng Z, et al. Expression of neuronal protein synuclein gamma gene as a novel marker for breast cancer prognosis. Breast Cancer Res Treat 2007;101:259–67.
23. Jiang Y, Liu YE, Goldberg ID, Shi YE. Gamma synuclein, a novel heat-shock protein-associated chaperone, stimulates ligand-dependant estrogen receptor alpha signaling and mammary tumorigenesis. Cancer Res 2004;64:4539–46.
24. Liu YE, Pu W, Jiang Y, Shi D, Dackour R, Shi YE. Chaperoning of estrogen receptor and induction of mammary gland proliferation by neuronal protein synuclein gamma. Oncogene 2007;26:2115–25.
25. Zhu Z, Friess H, diMola FF, et al. Nerve growth factor expression correlates with perineural invasion and pain in human pancreatic cancer. J Clin Oncol 1999;17:2419–28.
26. Zhu ZW, Friess H, Wang L, et al. Nerve growth factor exerts differential effects on the growth of human pancreatic cancer cells. Clin Cancer Res 2001;7:105–12.
27. Pan ZZ, Breuning W, Giasson BI, Lee VM, Godwin AK. Gamma-synuclein promotes cancer cell survival and inhibits stress- and chemotherapy drug-induced apoptosis by modulating MAPK pathways. J Biol Chem 2002;277:35050–60.
28. Surgucheva IG, Sivak JM, Fini ME, Palazzo RE, Surguchov AP. Effect of γ-synuclein overexpression on matrix metalloproteinases in retinoblastoma Y79 cells. Arch Biochem Biophys 2003;410:167–76.
29. Bloomston M, Zervos EE, Rosemurgy AS II. Matrix metalloproteinases and their role in pancreatic cancer: a review of preclinical studies and clinical trials. Ann Surg Oncol 2002;9:668–74.
30. Buchman VL, Adu J, Pinon LG, Ninkina NN, Davies AM. Persyn, a member of the synuclein family, influences neurofilament network integrity. Nat Neurosci 1998;1:101–3.
31. Maccioni RB, Cambiazo V. Role of microtubule-associated proteins in the control of microtubule assembly. Physiol Rev 1995;75:835–64.
32. Shen J, Person MD, Zhu J, Abbruzzese JL, Li D. Protein expression profiles in pancreatic adenocarcinoma compared with normal pancreatic tissue and tissue affected by pancreatitis as detected by two-dimensional gel electrophoresis and mass spectrometry. Cancer Res 2004;64:9018–26.
33. Bloomston M, Zhou JX, Rosemurgy AS, Frankel W, Muro-Cacho CA, Yeatman TJ. Fibrinogen γ overexpression in pancreatic cancer identified by large-scale proteomic analysis of serum samples. Cancer Res 2006;66:2592–9.
34. Iwaki H, Kageyama S, Isono T, et al. Diagnostic potential in bladder cancer of a panel of tumor markers (calreticulin, gamma-synuclein, and catechol-*o*-methyltransferase) identified by proteomic analysis. Cancer Sci 2004;95:955–61.

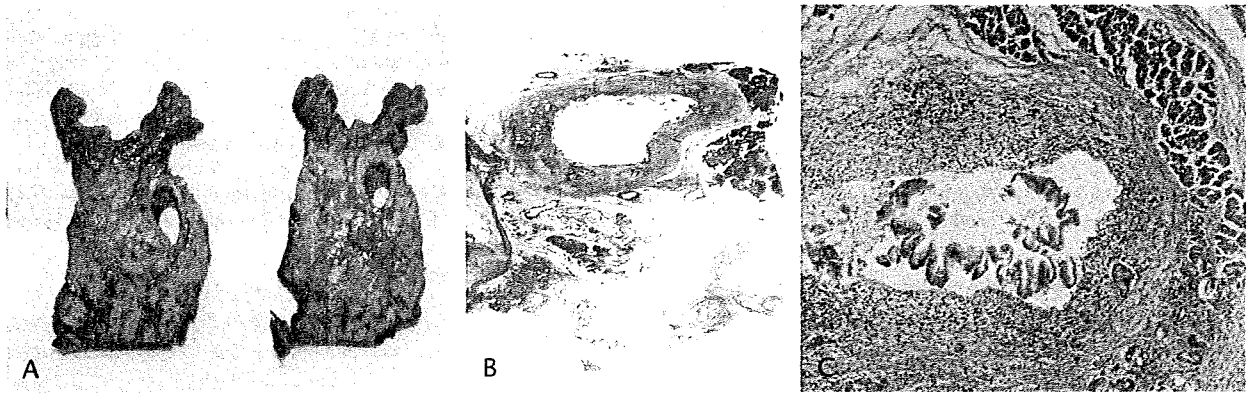

FIGURE 1. Resected specimen including pancreatic head (A). Pathological examination of the specimen showing sclerosing cholangitis of the intrapancreatic and extrapancreatic tracts of the CBD with mild to moderate dysplasia (B), lymphocytic and eosinophilic infiltrate, and multiple aspects of pancreatic intraepithelial neoplasia of 1-2-3 grades (C).

the gallbladder, and the CBD, were examined. Histopathological examination of the specimen showed sclerosing cholangitis of the intrapancreatic and extrapancreatic tracts of the CBD with mild to moderate dysplasia (Fig. 1B), eosinophilic enteritis, lymphoplasmacytic and eosinophilic infiltrate, and multiple aspects of pancreatic intraepithelial neoplasia of 1-2-3 grades (Fig. 1C). An eosinophilic infiltrate involving the gallbladder was also shown in the cholecystectomy specimen.

The main characteristics of AIP are as follows: (1) diffuse or segmental narrowing of the main pancreatic duct at imaging techniques, (2) increased levels of serum gamma-globulin or the presence of autoantibodies, and (3) the presence of fibrotic changes with lymphoplasmacytic cell infiltration around the main pancreatic duct. Diagnosis of autoimmune pancreatitis is established when criterion 1 together with criteria 2 and/or 3 are fulfilled. Clinically, however, the patient has a serrated stenosis of the third low of the CBD without evidence of major diagnostic criteria of AIP (preoperative imaging and presence of autoantibodies and hypergammaglobulinemia), and so we suspected a cancer of the lower bile duct. In addition, abnormal serum value of the tumor marker CA 19-9 was present. Even if it has been reported that approximately 50% of patients with autoimmune pancreatitis[6–8] may have abnormal serum levels of CA19-9, in our patient, the diagnosis of CBD cancer was made and we decided to operate him.

In conclusion, we have reported the first case of association of sclerosing cholangitis, autoimmune chronic pancreatitis, and situs viscerum inversus totalis.

Nicola Antonacci, MD
Riccardo Casadei, MD, PhD
Claudio Ricci, MD
Department of Surgery
University of Bologna
S. Orsola-Malpighi Hospital
Bologna, Italy
claudiochir@gmail.com
Raffaele Pezzilli, MD
Department of Internal Medicine
and Gastroenterology
University of Bologna
S. Orsola-Malpighi Hospital
Bologna, Italy
Lucia Calculli, MD
Department of Radiology
University of Bologna
S. Orsola-Malpighi Hospital
Bologna, Italy
Donatella Santini, MD
Department of Pathology
University of Bologna
S. Orsola-Malpighi Hospital
Bologna, Italy
Vincenzo Alagna, MD
Francesco Minni, MD, PhD
Department of Surgery
University of Bologna
S. Orsola-Malpighi Hospital
Bologna, Italy

REFERENCES

1. Nishino T, Toki F, Oyama H, et al. Biliary tract involvement in autoimmune pancreatitis. *Pancreas*. 2005;30(1):76–82.
2. Pezzilli R, Casadei R, Calculli L, et al. Autoimmune pancreatitis. A case mimicking carcinoma. *JOP*. 2004;5:527–530.
3. Hamano H, Kawa S, Uehara T, et al. Immunoglobulin G_4–related lymphoplasmacytic sclerosing cholangitis that mimics infiltrating hilar cholangiocarcinoma: part of a spectrum of autoimmune pancreatitis? *Gastrointest Endosc*. 2005;62:152–157.
4. Quintini C, Buniva P, Farinetti A, et al. Adenocarcinoma of pancreas with situs viscerum inversus totalis. *Minerva Chir*. 2003;58(2):243–246.
5. Sakaguchi O, Kamio H, Sakurai H, et al. Pancreas head carcinoma associated with situs inversus viscerum totalis. *Nippon Geka Gakkai Zasshi*. 1985;86(1):111–115.
6. Takikawa H, Takamori Y, Tanaka A, et al. Analysis of 388 cases of primary sclerosing cholangitis in Japan; presence of a subgroup without pancreatic involvement in older patients. *Hepatol Res*. 2004;29(3):153–159.
7. Hirano K, Shiratori Y, Komatsu Y, et al. Involvement of the biliary system in autoimmune pancreatitis: a follow-up study. *Clin Gastroenterol Hepatol*. 2003;1(6):453–464.
8. Kamisawa T, Tu Y, Egawa N, et al. Involvement of pancreatic and bile ducts in autoimmune pancreatitis. *World J Gastroenterol*. 2006;12(4):612–614.

Slow Growth of Small Pancreatic Carcinoma With a 20-Month Follow-Up

To the Editor:

Invasive ductal adenocarcinoma of the pancreas has a poor prognosis mainly because of rapid progressive growth beyond the pancreas and a tendency to demonstrate early metastasis to the regional lymph nodes.[1] An evaluation of the growth rate of pancreatic carcinoma is essential to predict the efficacy of treatment and the prognosis. The growth rate of pancreatic carcinoma has been described in patients

with liver metastases or with far advanced stages, including unresectable patients.[2,3] However, there has so far been no report concerning the growth rate of small pancreatic cancers. In this report, we describe a small pancreatic cancer, which grew from 12 mm to 30 mm in maximum diameter serially measured by ultrasonography (US), with a follow-up period of 20 months.

CASE REPORT

A 63-year-old woman received an annual health checkup, without any specific symptoms, in February 2006. Ultrasonography (US) revealed a 12-mm hypoechoic mass in the pancreatic head, with no dilation of the main pancreatic duct (Fig. 1A). She had no history of diabetes mellitus or alcohol abuse. The physical examination was unremarkable. The serum levels of carcinoembryonic antigen and carbohydrate antigen 19-9 (CA19-9) were within the reference ranges. Computed tomography (CT) and magnetic resonance imaging demonstrated a well-demarcated and enhanced 12-mm tumor. Contrast-enhanced CT during the late phase showed a small hyperattenuating lesion in the pancreatic head (Fig. 1B). Under a provisional diagnosis of pancreatic head cancer or islet cell tumor, a pylorus-preserving pancreaticoduodenectomy was thus strongly recommended. However, the patient refused to undergo surgical treatment without a definitive diagnosis of malignancy. Consequently, a fine-needle aspiration biopsy was obtained, and the tumor was diagnosed as suggestive of an islet cell tumor.

During the follow-up, the tumor gradually increased in maximum diameter, measuring 30 mm with 5-mm dilation of the main pancreatic duct by US (Fig. 1C) in October 2007. The value of CA19-9 also increased to 113 U/mL in September 2007. The maximum diameter of the tumor by US (Fig. 2A) and the value of CA19-9 level (Fig. 2B) were serially measured at almost the same time. A mean growth rate of 0.9 mm per month was calculated. The tumor volume doubling time (TVDT)[4] and the CA19-9 doubling time were 152 and 276 days, respectively.

In October 2007, a pancreaticoduodenectomy was performed on the diagnosis of pancreatic head carcinoma because of the progressive tumor growth. The cut surface of the resected tumor was well demarcated and grayish-white. The macroscopic appearance was a nodular type, which histopathologically measured 18 mm × 18 mm × 15 mm in size (Fig. 2C). The TVDT based on the tumor diameter was histopathologically confirmed to be 341 days. Obstructive pancreatitis was observed just distal to the tumor. Most of the tumor was confined to the pancreas, but it slightly invaded the retroperitoneal fat tissue near the gastroduodenal artery, but no invasion of the bile duct, duodenum, and adjacent large vessels was observed. The pathological examination of the tumor revealed a well to moderately differentiated tubular adenocarcinoma of the pancreas (Fig. 2D). This carcinoma formed mainly irregular papillotubular patterns accompanied by a desmoplastic stroma. The morphological structures clearly demonstrated a typical ductal adenocarcinoma of the panccreas. There was slight lymphatic and intrapancreatic nerve invasion, but no venous invasion. Node involvement was absent in the 19 harvested lymph nodes, and all of the resection margins were negative.

The postoperative course was uneventful. The patient is doing well without recurrence at 3 months after the operation.

DISCUSSION

Even with a sophisticated imaging assessment, the precise preoperative

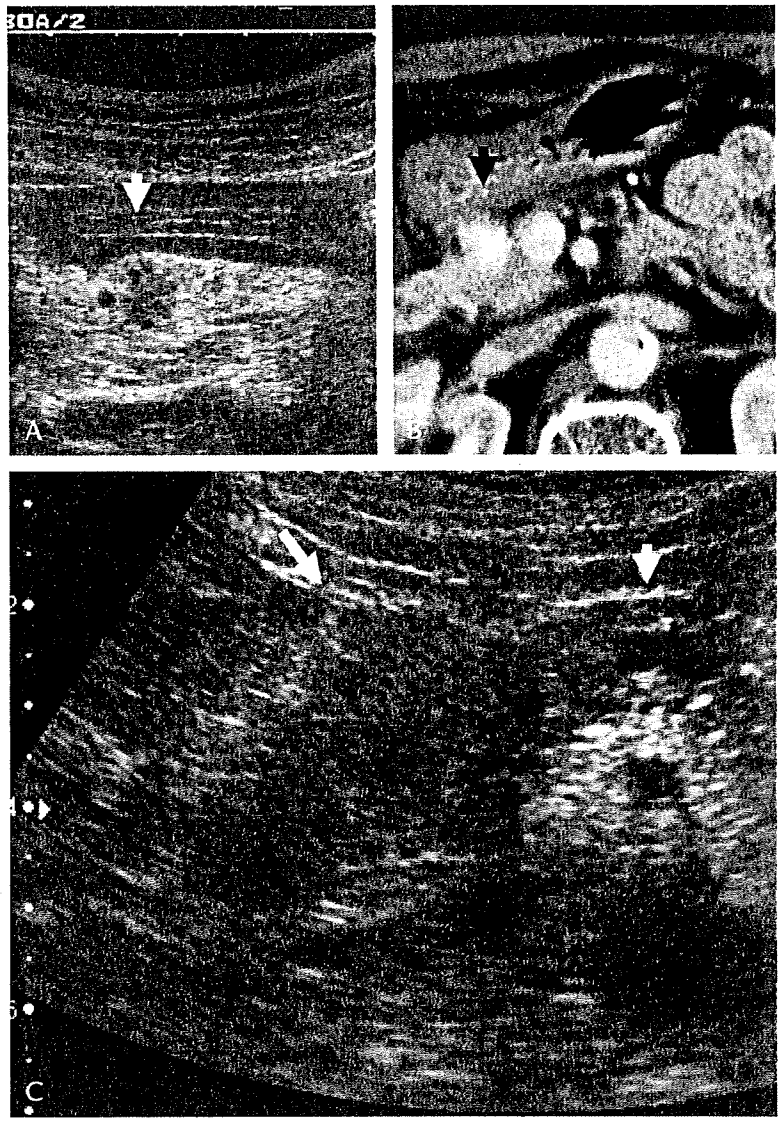

FIGURE 1. A, The US shows a small low-echoic mass measuring 12 mm in size. The white arrow indicates a small tumor. B, Enhanced CT in the late phase shows a round hyperattenuating lesion in the pancreatic head. The black arrow indicates a small tumor. C, The US shows a low-echoic mass 30 mm in diameter, with dilation of the main pancreatic duct. The white arrow indicates a tumor, and the black one the dilated main pancreatic duct.

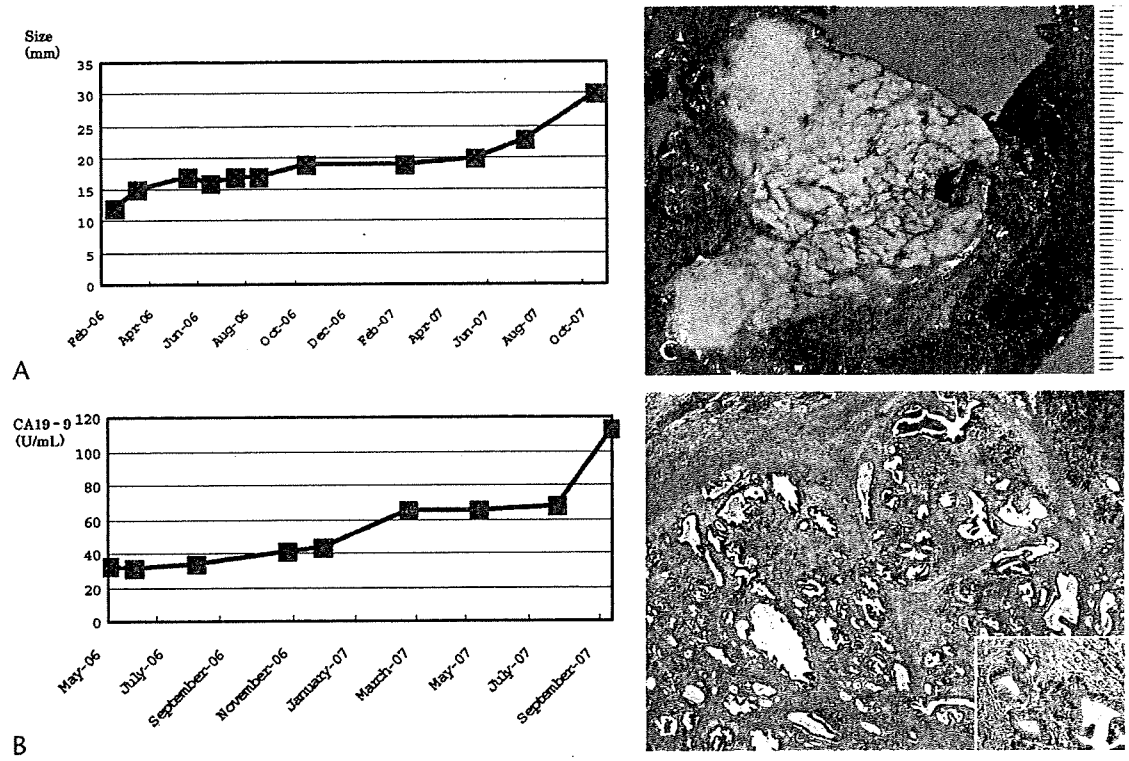

FIGURE 2. A, The maximum tumor size serially measured by US over time. B, The CA19-9 serially measured during the follow-up period. C, The macroscopic appearance shows a nodular-type tumor, histopathologically measured at 18 mm in maximum diameter. D, The histological appearance of the pancreatic lesion (hematoxylin-eosin, original magnification ×25). The morphological appearance is typical of pancreatic ductal carcinoma with irregular papillotubular patterns accompanied by a desmoplastic stroma. Inset: A higher magnification shows a well to moderately differentiated tubular adenocarcinoma of the pancreas (hematoxylin-eosin, original magnification ×100).

diagnosis of small pancreatic lesions has been challenging.[5,6] It has at times been difficult to obtain a cytological diagnosis using fine-needle biopsy in pancreatic lesions measuring less than 20 mm in diameter.[7] Fundamentally, a surgical resection should be recommended, but the present patient refused surgical treatment because of the lack of a definitive diagnosis. In the current case, the pancreatic tumor gradually increased from 12 mm up to 30 mm as measured by US, but the histopathologic measurement disclosed 18 mm in maximum diameter. The TVDT measured by US was 152 days, but that on the basis of the histopathologic measurement was 341 days. Furukawa et al[3] described the TVDT in 9 patients with primary pancreatic carcinoma to range from 64 to 255 days. This tumor, most of which was confined to the pancreas without nodal involvement, had a slow-growing nature, although the pathological findings were typical of pancreatic carcinoma. The mode of progression or growth rate of advanced pancreatic carcinomas,[2,3] intraductal papillary-mucinous tumor,[8] and other low-grade malignant lesions[9] have been previously described, but to our knowledge, the growth rate of small pancreatic carcinomas has not yet been reported. The measurement of the growth rate of a small pancreatic carcinoma might be extremely difficult because many patients with a tiny cancer have negative imaging findings, with only a dilation of the main pancreatic duct.[5]

A well-demarcated tumor with homogeneous vascularity is one of the major characteristics of the islet cell tumor.[6] On the contrary, the concomitant dilation of the main pancreatic duct is a principal finding in differentiating the small pancreatic cancer. Yang et al[6] revealed that 5patients (5/32, 15.6%) with pancreatic carcinoma showed a homogeneous enhancing pattern on contrast-enhanced US. Only 1 patient with an islet cell tumor located in the pancreatic head had ductal dilation. In the current case, imaging studies and fine-needle aspiration biopsy cytology could not provide a precise diagnosis. Regardless, a close follow-up study was indispensable when surgical treatment could not be pursued. We recommend such a patient to receive a US examination and a CA19-9 test at least every 2 to 3 months.

The precise tumor size measurement before resection is difficult because the boundary between the pancreatic carcinoma and the noncancerous parenchyma is usually irregular and indistinct because of the cancer's invasive growth. The tumor size measured by US was extensively larger than the tumor size confirmed by the histopathologic examination. The reason might be because of an inflammatory reaction around the tumor, with concomitant pancreatitis caused by the progressive increase of the tumor. Furukawa et al[10] recommended tumor size measurement by dynamic CT because there was a significant correlation between the tumor size as determined by dynamic CT and that on the histopathologic examination, especially in small tumors.

The current case disclosed an unexpected slow growth, but no specific clinical factors that could explain the slow growth of the tumor were observed besides a well-demarcated structure with a homogeneous hyperattenuating nature. The growth rate of small pancreatic carcinomas

is a great clinical concern because it is important to collect enough cases to evaluate the relationship between the growth speed of the small pancreatic carcinoma and the screening and diagnostic procedures, pathological factors, and prognosis.

ACKNOWLEDGMENTS

This study was supported by a grant-in-aid for cancer research from the Ministry of Health, Labour and Welfare of Japan.

The authors have no direct or indirect commercial and financial incentive associated with publishing the article.

Kazuaki Shimada, MD
Department of Hepatobiliary and Pancreatic Surgery
National Cancer Center Central Hospital
Tokyo, Japan
kshimada@ncc.go.jp

Hiroaki Onaya, MD
Clinical Trials and Practice Support Division
Center for Cancer Control and Information Service
National Cancer Center
Tokyo, Japan

Minoru Esaki, MD

Yoshihiro Sakamoto, MD

Satoshi Nara, MD

Tomoo Kosuge, MD
Department of Hepatobiliary and Pancreatic Surgery
National Cancer Center Central Hospital
Tokyo, Japan

Yasunori Mizuguchi, MD
Diagnostic Radiology Division
National Cancer Center Central Hospital
Tokyo, Japan

Nobuyoshi Hiraoka, MD
Pathology Division
National Cancer Center Research Institute
Tokyo, Japan

REFERENCES

1. Shimada K, Sakamoto Y, Sano T, et al. Reappraisal of the clinical significance of tumor size in patients with pancreatic ductal carcinoma. *Pancreas.* 2006;33:233–239.
2. Amikura K, Kobori M, Matsuno S. The time of occurrence of liver metastasis in carcinoma of the pancreas. *Int J Pancreatol.* 1995;17:139–146.
3. Furukawa H, Iwata R, Moriyama N. Growth rate of pancreatic adenocarcinoma: initial clinical experience. *Pancreas.* 2001;22:366–369.
4. Collins VP, Loeffler RK, Tivey H. Observation of growth rates of human tumors. *AJR Am J Roentgenol.* 1956;76:988–1000.
5. Ishikawa O, Ohigashi H, Imaoka S, et al. Minute carcinoma of the pancreas measuring 1 cm or less in diameter—collective review of Japanese case reports. *Hepatogastroenterology.* 1999;46:8–15.
6. Yang W, Chen MH, Yan K, et al. Differential diagnosis of non-functional islet tumor and pancreatic carcinoma with sonography. *Eur J Radiol.* 2007;62:342–351.
7. Shin HJC, Lahoti S, Sneige N. Endoscopic ultrasound–guided fine-needle aspiration in 179 cases. The M. D. Anderson Cancer Center experience. *Cancer Cytopathology.* 2002;96:174–180.
8. Kobayashi G, Fujita N, Noda Y, et al. Mode of progression of intraductal papillary-mucinous tumor of the pancreas: analysis of patients with follow-up by EUS. *J Gastroenterol.* 2005;40:744–751.
9. Spinelli KS, Fromwiller TE, Daniel RA, et al. Cystic pancreatic neoplasms: observe or operate. *Ann Surg.* 2004;239:651–659.
10. Furukawa H, Takayasu K, Mukai K, et al. Computed tomography of pancreatic adenocarcinoma: comparison of tumor size measured by dynamic computed tomography and histopathologic examination. *Pancreas.* 1996;13:231–235.

A Case of Squamoid Cyst of Pancreatic Ducts

To the Editor:

Detection of cystic lesions in the pancreas has increased because of the widespread use of high-resolution diagnostic imaging techniques. Therefore, cystic lesion of the pancreas constitutes an increasingly important category with a challenging differential diagnosis.[1] Squamoid cyst of pancreatic ducts is a recently recognized type of cystic lesion in the pancreas in which cystically dilated ducts are lined by nonkeratinized squamous epithelium.[2] Clinically, it is important to distinguish this generally benign cystic lesion from the potentially malignant mucinous cyst-forming neoplasias, especially mucinous cystic neoplasms (MCNs) and intraductal papillary mucinous neoplasms (IPMNs). We report the first case of squamoid cyst of pancreatic ducts in Japan.

CASE REPORT

An 80-year-old man underwent an abdominal computed tomography (CT) for routine follow-up postrectal cancer surgery; a 2.0-cm cystic lesion was detected in the body of the pancreas. At 16 months of follow-up, the size of the cystic lesion had increased to 3.0 cm and the patient was admitted to our hospital for further examinations. Inpatient evaluation revealed no symptoms related to the lesion. The patient's abdomen was soft and flat, and no pressure pain was observed. Complete blood count, electrolytes, and liver function tests were all normal. There were no data to indicate pancreatitis. Both serum carbohydrate antigen 19-9 and carcinoembryonic antigen levels were normal.

A contrast-enhanced multidetector-row CT showed a well-demarcated, low-attenuating cystic lesion in the body of the pancreas. The lesion measured 3.1 × 2.4 cm and had several small calcifications. There were no indications of invasion into the surrounding tissues or dilatation of the main pancreatic duct (Fig. 1A). Magnetic resonance cholangiopancreatography revealed a 3-cm round cystic lesion in the pancreatic body, which did not communicate with the main pancreatic duct. The main pancreatic duct was not dilated (Fig. 1B). Abdominal ultrasound (US) showed a cystic lesion with clear margins and a smooth surface that contained several echogenic solid processes and small intraluminal calcifications (Fig. 1C). Endoscopic US revealed that the cystic lesion was divided into several cysts by thin septa and that the lesion contained several 6- to 12-mm solid processes within the lumina of the cysts (Fig. 1D).

We diagnosed the cystic lesion as MCN and performed laparotomy. Intraoperatively, the cystic lesion, approximately 3 cm in diameter, was palpated arising from the body of the pancreas without any infiltration into the surrounding tissues. Most of the lesion was intrapancreatic, and its border was well defined. There was no peripancreatic lymph node swelling. Therefore, we performed a central pancreatectomy. The patient had an uneventful postoperative course and was discharged 17 days after surgery. The patient quickly returned to his normal activities.

Macroscopically, the cystic lesion of the pancreas (3.1 × 2.4 cm) was multilocular with thin septa. There were several elastic, hard, white lumps within the lumina, and the central portions of the relatively large lumps were particularly hard (Fig. 1E). The cystic lesion contained serous clear fluid. Histologic examination revealed that the cysts had variable linings ranging from flat squamoid cell to transitional, to stratified squamous without keratinization. No tall columnar mucinous cells were identified. No associated lymphoid or splenic tissue was present. The cyst walls were composed of relatively thin fibrous tissue. None of the lesions displayed ovarianlike stroma. The white

Surg Today (2009) 39:32–37
DOI 10.1007/s00595-008-3814-7

SURGERY TODAY

Roux-en-Y Reconstruction Using Staplers During Pancreaticoduodenectomy: Results of a Prospective Preliminary Study

YOSHIHIRO SAKAMOTO, TAKAHIRO KAJIWARA, MINORU ESAKI, KAZUAKI SHIMADA, SATOSHI NARA, and TOMOO KOSUGE

Hepatobiliary and Pancreatic Surgery Division, National Cancer Center Hospital, 5-1-1 Tsukiji, Chuo-ku, Tokyo 104-0045, Japan

Abstract

Purpose. The aim of this study was to reveal the utility of alimentary reconstruction using staplers during pancreaticoduodenectomy (PD), focusing on the occurrence of delayed gastric emptying.

Methods. Between 2003 and 2007, 72 PDs with alimentary reconstruction were performed by a single surgeon. Since August 2006, the new Roux-en-Y reconstruction methods using staplers were applied in 26 of the patients. We compared their clinical outcomes with those of the 46 patients who underwent PD using the conventional hand-sewn reconstruction methods.

Results. The results of upper gastrointestinal study showed improvement within 10 postoperative days (PODs; $P = 0.03$): the patients resumed eating their regular diet sooner (13 vs 6 days, $P < 0.001$), and both the incidence of delayed gastric emptying (43% vs 19%, $P = 0.04$) and the hospital stay (27 vs 21 days, $P = 0.008$) were reduced significantly in patients with stapled reconstruction. Despite the fact that operative costs were significantly higher for patients with stapled reconstruction ($P = 0.009$), hospital costs were significantly lower ($P = 0.049$) for those who underwent the conventional method.

Conclusions. Our retrospective analysis shows that stapled reconstructions might reduce the incidence of delayed gastric emptying; however, further study will be necessary to evaluate the utility of this new method.

Key words Pancreaticoduodenectomy · Delayed gastric emptying · Stapled reconstruction · Roux-en-Y reconstruction · Hospital stay

Reprint requests to: Y. Sakamoto
Received: April 2, 2008 / Accepted: May 28, 2008

Introduction

Alimentary reconstruction using staplers during gastric and colorectal surgery is widely accepted. The use of circular staplers in esophagojejunostomy is more convenient and safer than hand-sewn suturing.[1] Moreover, colorectal anastomoses using a double stapling technique have also become popular,[2] especially since the advent of laparoscopic surgery.[3] However, to our knowledge, mechanical reconstruction using staplers during pancreatectomy has never been documented.

One of the most common complications of pancreaticoduodenectomy (PD) is delayed gastric emptying (DGE), otherwise known as "gastroparesis,"[4] which is not fatal but results in prolonged hospital stay and increased hospital costs. Delayed gastric emptying is defined as nasogastric decompression after postoperative day (POD) 10 or a failure to tolerate a regular diet after POD 14. The incidence of DGE has been reported to range from 5% to 72%.[5–13] We hypothesized that the hand-sewn, two-layered, or continuous suture could induce anastomotic edema, which is one of the causes of DGE. Mechanical alimentary reconstruction can prevent anastomotic edema and may keep the oral intake stable. Therefore, in August 2006, we introduced a new Roux-en-Y reconstruction method, which uses circular or linear staplers during PD. We report the preliminary results of our new method.

Patients and Methods

Between August 1, 2003 and September 30, 2007, 302 patients underwent PD in our institute. These operations were performed by one or more of five surgeons, so to maintain consistency we evaluated the surgical outcomes of the 76 PDs performed by a single surgeon (Y.S.). Between August 2003 and July 2006, 50 patients underwent PD with alimentary reconstruction using the

conventional hand-sewn method. The new stapled Roux-en-Y reconstruction method was introduced in August 2006, and 26 patients underwent mechanical reconstruction in the final year of the study. Among the 50 patients operated on during the former 3 years, the following four patients were excluded from the analysis: two who had undergone previous gastrojejunostomy, one who had undergone previous total gastrectomy, and one who underwent PD concomitant with total gastrectomy.

The underlying diseases were as follows: invasive pancreatic cancer in 41 patients, bile duct cancer in 12 patients, ampullary cancer in 7 patients, intraductal papillary mucinous tumor in 3 patients, neuroendocrine tumor in 2 patients, metastatic cancers in 2 patients, duodenal cancer in 1 patient, and other noncancerous diseases in 4 patients. The surgical procedures consisted of standard Whipple procedure (SW) in 22 patients and pylorus-preserving pancreaticoduodenectomy (PPPD) in 50 patients. Twenty patients (28%) underwent combined portal vein resection. One patient underwent concomitant extended right hemihepatectomy, and another underwent concomitant distal pancreatectomy.

The surgical outcomes of PD, including the occurrence of DGE and other surgical complications, were compared between the 46 patients who underwent PD using conventional reconstruction and the 26 patients who underwent the new Roux-en-Y stapled reconstruction. The backgrounds and surgical procedures of each group are summarized in Table 1.

Surgical Technique of PD

The details of the standard procedure for PD have been described elsewhere.[14] After removal of the pancreatic head, we wrapped the stump of the gastroduodenal artery using the falciform ligament to prevent the bleeding caused by pancreatic leakage.[15] A jejunal loop was lifted and pancreaticojejunostomy was performed by duct-to-duct anastomosis using 5-0 polydioxanone (PDS). The anterior and posterior pancreatic walls were tightly affixed to the jejunal serosa using interrupted 4-0 PDS sutures. A hepaticojejunostomy was then done using interrupted 5-0 PDS sutures.

Conventional Reconstruction

In the 46 conventional PDs, we performed an antecolic gastrojejunostomy and duodenojejunostomy during the standard Whipple procedure (SW, $n = 16$) and pylorus-preserving pancreaticoduodenectomy (PPPD, $n = 30$), respectively. These anastomoses were done on antecolic routes, by the Albert–Lembert ($n = 38$), layer to layer ($n = 6$), or Gambee ($n = 2$) methods. A Braun jejunojejunostomy was done to prevent direct exposure of the anastomotic site to pancreatic and bile juice. Gastric tubes ($n = 43$) and jejunal feeding tubes ($n = 45$) were pulled out through the afferent loop between the duodeno- or gastrojejunostomy and Braun anastomosis. External drainage of the pancreatic and biliary ducts was performed in all of the patients.

Roux-en-Y Reconstruction Using a Circular Stapler During Pylorus-Preserving Pancreaticoduodenectomy (PPPD)

An antecolic duodenojejunostomy was performed by Roux-en-Y reconstruction using a circular stapler in 20 PPPDs (Proximate ILS 29 or 25 mm, Ethicon Endo-Surgery, Cincinnati, OH [$n = 19$], EEA circular stapler,

Table 1. Clinical characteristics of patients who underwent conventional versus Roux-en-Y stapled reconstruction

	Conventional ($n = 46$)	Roux-en-Y, stapled ($n = 26$)	P value
Sex			
Male	29	15	0.66
Female	17	11	
Age (years)	68 (18–82)	66 (47–80)	0.80
Body mass index	21 (15–28)	22 (17–27)	0.25
Diseases			
Pancreatic cancer	26	15	0.81
Bile duct cancer	7	5	
Vater or duodenal cancer	7	2	
Others	6	4	
Procedure			
SW	16	6	0.30
PPPD	30	20	
Portal vein resection			
Performed	14 (30%)	6 (23%)	0.50
Operative time (min)	560 (400–842)	570 (374–790)	0.77
Blood loss (ml)	850 (215–2360)	710 (130–2420)	0.19

SW, standard Whipple procedure; PPPD, pylorus-preserving pancreaticoduodenectomy

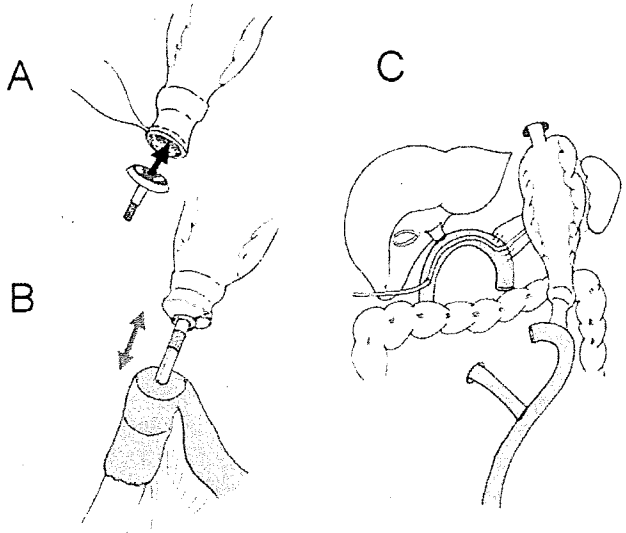

Fig. 1A–C. Schematic illustration of Roux-en-Y duodenojejunostomy using a circular stapler. **A** A purse-string suture was placed around the duodenal stump, and an anvil was placed within. **B** Duodenojejunostomy was accomplished using a circular stapler. **C** Pancreaticojejunostomy, hepaticojejunostomy, and Roux-en-Y duodenojejunostomy with an external pancreatic drainage

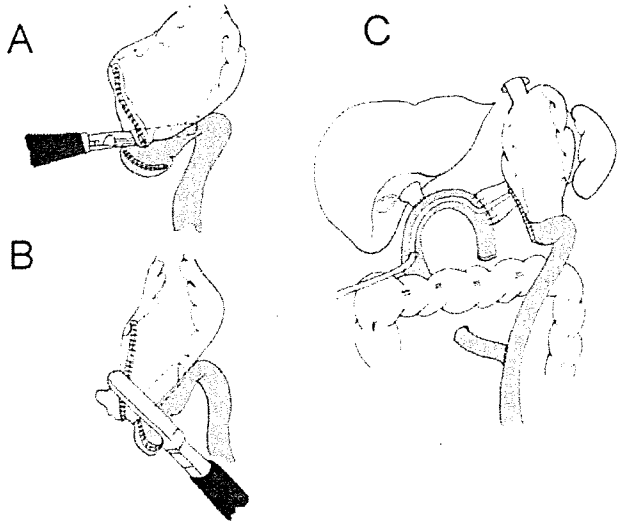

Fig. 2A–C. Schematic illustration of Roux-en-Y gastrojejunostomy using linear staplers. **A** Gastrojejunostomy using a linear stapler. A side-to-side anastomosis was made between the posterior wall of the stomach and the side wall of the jejunum. **B** The edges of the stomach and the jejunal loop were divided using a linear stapler. **C** Pancreaticojejunostomy, hepaticojejunostomy, and Roux-en-Y gastrojejunostomy with an external pancreatic drainage

28 mm, US Surgical, Norwalk, CT [n = 1]) (Fig. 1). The duodenum was divided 3–4 cm anal of the pylorus ring. A segmental jejunum was sacrificed and resected, preserving the mesojejunum, and the anal jejunum was used for the duodenojejunostomy. An anvil device was inserted into the duodenal stump, a circular stapler was inserted into the jejunal loop, and the mechanical anastomosis was completed. The stump of the jejunal loop was closed using a linear stapler.

Roux-en-Y Reconstruction Using a Linear Stapler During Standard Whipple Procedure (SW)

In four SWs an antecolic gastrojejunostomy was performed by Roux-en-Y reconstruction using a linear stapler (Endo-GIA Reticulator 60, US Surgical) (Fig. 2). A segmental jejunum was removed, preserving the mesojejunum, and the anal jejunum was used for the gastrojejunostomy. A small incision was made on the posterior wall of the stomach, near the stump on the greater curvature. A linear stapler was inserted into the remnant stomach and the jejunum to adjust the posterior wall of the stomach and the side wall of the jejunum. A mechanical anastomosis was made, and the stumps of the stomach and the jejunum were closed using another linear stapler.

In the remaining two PDs, a circular stapler was used to make a gastrojejunostomy on the posterior wall of

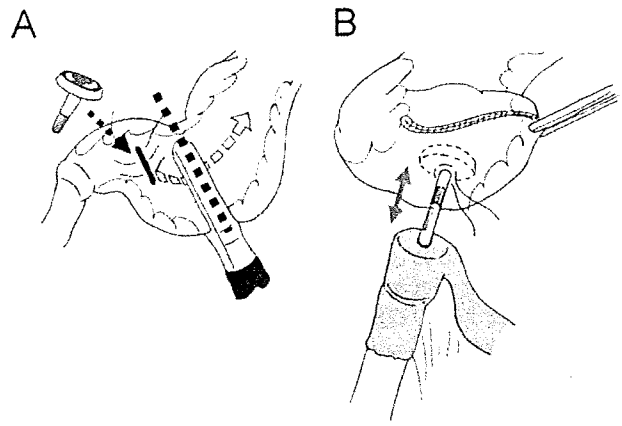

Fig. 3A,B. Schematic illustration of Roux-en-Y gastrojejunostomy using a circular stapler. **A** The anvil was inserted through a small incision in the antrum into the fornix of the stomach. The incision was closed with interrupted sutures. **B** The handle of the anvil was pulled out though the posterior wall of the stomach, and the root of the handle was closed using a purse-string suture. Thereafter, a gastrojejunostomy was accomplished using the circular stapler

the stomach (Fig. 3). Before dividing the stomach during SW the anvil was inserted into the fornix of stomach through a small incision in the antrum, which was then sutured. The handle of the anvil was pulled out of the posterior wall of the remnant stomach, and a mechani-

cal anastomosis was completed. The stump of the jejunum was closed using another linear stapler.

In both the mechanical Roux-en-Y reconstructions during PPPD and SW, the anal jejunojejunostomy was created by serosa-to-serosa continuous suture. Gastrostomy was not done in any of the patients. In the pancreaticojejunostomy, an internal stent (n = 5) or an external drainage tube (n = 19) was placed in 24 patients. In the hepaticojejunostomy, an internal stent (n = 16) or external drainage tube (n = 2) was placed in 18 patients. In 23 patients a jejunal drainage tube (n = 8) to decompress the anastomotic loop or a jejunal feeding tube (n = 15) was inserted through the right-sided jejunal loop. The nasogastric tube was removed on POD 1 in all 26 patients. Two closed drains were inserted beside the pancreaticojejunostomy, and intermittent suction was applied 24 h a day for 4–6 days in the former term. In the latter 2 years, intermittent suction was not used. Patients were discharged home when they were able to resume eating about half the amount of their regular diet and had only minimal output from one abdominal drain.

Definition of Outcome Measures

The results of the upper gastrointestinal (UGI) study were evaluated within 10 PODs according to the degree of passage of the contrast medium. Grade A showed good passage of the medium without any dilatation of the stomach; grade B showed mild dilatation of the remnant stomach or formation of the niveau in the stomach, and passage of the medium could be maintained when the patient leaned forward; and grade C showed severe dilatation of the remnant stomach or no passage of the contrast medium.

Delayed gastric emptying was defined as failure to start a regular diet within 14 PODs according to previous reports.[5,6,9–11,13] Postoperative pancreatic fistula was graded according to the definitions proposed by an international study group on pancreatic fistula,[16] namely, when the amylase concentration of the drain fluid obtained on, or after POD 3 was greater than three times the serum amylase concentration. Pancreatic fistulas were classified into grades A, B, and C according to severity; grade A was a "transient fistula," not associated with a delay in hospital discharge; a grade B fistula led to a delay in discharge, with persistent drainage for more than 3 weeks; and a grade C fistula was usually associated with major complications. Grades B and C fistula were considered to be major complications.

Comparison of the Two Reconstruction Methods

We compared the operative times, blood loss, results of the UGI study, morbidity and mortality, and operative and hospital costs between the patients who underwent conventional reconstruction and those who underwent the stapled Roux-en-Y reconstruction.

Statistical Analysis

Statistical analysis was done using the chi-square test or Fisher's exact test for univariate analysis. We used the Mann–Whitney U-test to compare the variables between the two groups. Data are expressed as medians and ranges. A P value of less than 0.05 was considered significant.

Results

There was no in-hospital mortality (0%) and the overall morbidity rate was 63%. Pancreatic fistula developed in 33 (46%) patients (grade A in 12, grade B in 20, and grade C in 1) and was clinically significant in 29%. Twenty-five (35%) patients suffered DGE. Major morbidity included grade C pancreatic fistula in one patient, who suffered sepsis and required percutaneous drainage of the abdominal fluid under computed tomography (CT) guidance. Another major morbidity was anastomotic bleeding after stapled reconstruction, which resulted in shock status of the patient on POD 16. Three other patients suffered bleeding from the stapled anastomotic site: on POD 1 in one and on POD 2 in two. The bleeding was indicated by decreased hematocrit levels as the patients' general condition was stable. All three underwent endoscopic clipping of the bleeding points, and recovered conservatively. None of the patients suffered arterial bleeding associated with the pancreatic fistula.

There were no remarkable differences in the patients' backgrounds, operative parameters, incidence of pancreatic fistula, or overall morbidity rates between the patients who underwent conventional reconstruction and those who underwent Roux-en-Y stapled reconstruction (Table 1). Gastrostomy was not done in the stapled reconstruction group patients, but none of these patients required reinsertion of a nasogastric tube. The results of the UGI study were significantly better in the 26 patients with stapled reconstruction than in the 43 patients who underwent conventional reconstruction (P = 0.03). The exception was the median duration between surgery and the UGI study, which was significantly longer in the conventional reconstruction group than in the stapled reconstruction group (6 days vs 5 days, $P < 0.001$). The duration between surgery and start of oral intake, the incidence of DGE, and the hospital stay were significantly reduced in the stapled reconstruction group vs. the conventional reconstruction group ($P < 0.001$, P = 0.04, and P = 0.008, respectively). The opera-

Table 2. Operative outcomes of patients who underwent conventional reconstruction versus Roux-en-Y stapled reconstruction

	Conventional ($n = 46$)	Roux-en-Y, stapled ($n = 26$)	P value
Removal of nasogastric tube or closure of gastrostomy (POD)	6	1	<0.001*
Results of UGI study ≤10 PODs			
Grade A	22	20	0.03*
Grade B or C	21	6	
Day of UGI study	6 (4–10)	5 (3–9)	<0.001*
Resumption of regular diet (POD)	13 (5–62)	6 (4–20)	<0.001*
DGE			
Absent	26	21	0.04*
Present	20	5	
Pancreatic fistula			
None, Grade A	34	17	0.44
Grade B or C	12	9	
Placement of drains	13 (6–72)	11 (2–65)	0.08
Minor complications	27	16	0.81
Major complications	1	1	0.68
Hospital stay (days)	27 (14–89)	21 (10–37)	0.008*
Operative costs ($)	8000	8700	0.009*
Hospital costs ($)	18000	17000	0.049*
Mortality	0	0	ND

UGI, upper gastrointestinal; POD, postoperative days; DGE, delayed gastric emptying; ND, not determined
* $P < 0.05$

tive costs were US$700 higher ($P = 0.009$), but the hospital cost was significantly ($1000) lower ($P = 0.049$) in the stapled reconstruction group than in the conventional group (Table 2).

Discussion

The findings of the present study suggest that the new Roux-en-Y reconstruction, using circular or linear staplers during PD, might improve the early passage of duodenojejunostomy and gastrojejunostomy, and thereby reduce the incidence of DGE. The stapled anastomosis felt very neat to the touch, which might contribute to preventing postoperative anastomotic edema. In addition, Roux-en-Y reconstruction would eradicate bile reflux and position the stomach tube vertically; thereby potentially assisting in advancing the stomach contents.[11] The incidence of anastomotic bleeding in this initial study (15%) was unexpectedly higher than that after gastric or colorectal surgery. Anastomotic bleeding was a major drawback in stapled reconstruction, so we strongly recommend confirming hemostasis of the anastomotic site via the jejunal loop and administering proton pump inhibitors postoperatively. Furthermore, we hope that the quality of staplers will improve in the future.

The passage of contrast medium in the UGI study and the recommencement of oral intake were improved significantly ($P = 0.03$ and < 0.001, respectively) and the incidence of DGE was reduced significantly ($P = 0.04$) by the introduction of stapled reconstruction (Table 2). Delayed gastric emptying has been reported to be affected by several other factors including gastric dysrhythmias due to intra-abdominal complications,[5,6] gastric atony after duodenal resection in response to the reduction of motilin,[7,17] pylorospasm secondary to vagotomy,[8] and angulation of the reconstructed alimentary tract.[18] A prospective randomized trial showed that erythromycin,[7] cyclic enteral feeding,[9] and antecolic reconstruction[10] all reduced DGE, whereas a retrospective study showed that ante-mesenteric reconstruction,[6] vertical reconstruction,[11] and straight-lined antecolic reconstruction[12] improved the oral intake. However, to our knowledge, the present study is the first to show the possible advantages of stapled Roux-en-Y reconstruction during PD.

This study is a retrospective analysis of one surgeon's experience. During the initial 3 years, oral intake was resumed very late, partly because we feared early bleeding, which might evoke pancreatic fistula. Since the introduction of stapled reconstruction in August 2006, the incidence of pancreatic fistula has been gradually decreasing, probably as a result of the improved surgical skill in pancreaticojejunostomy during PD. Fortunately, since the introduction of internal stents in pancreaticojejunostomy and in hepaticojejunostomy, external drainage is no longer needed. This may contribute to early discharge from hospital. Gastrostomy was placed in 97% of the patients who underwent the conventional

method, but it was not required in any of those who underwent stapled reconstruction. This strongly affected the duration of gastric decompression. The difference in hospital stay between the two groups may be reflected not only by the methods of alimentary reconstruction, but also by the placement of drainage or feeding tubes, and management of drainage tubes. A multi-institutional prospective randomized trial will be necessary to evaluate the efficiency of this stapled reconstruction during PD.

The possible advantages of the Roux-en-Y stapled reconstruction we described are as follows: standardization of reconstruction, irrespective of the attending surgeon; easy reconstruction; possible prevention of anastomotic edema and subsequent stricture, brought about by continuous two-layer anastomosis; and a complete diversion of the bile and pancreatic juice from the anastomosis. On the other hand, its disadvantages are as follows: higher cost; a risk of bleeding at the anastomotic site; and mass production of industrial waste. It is noteworthy that the operative costs were higher in the stapled group, but the overall hospital costs were higher in the conventional method group. This is most likely due to the reduced costs for hospital stay and nutritional support required in the stapled group.

In conclusion, our retrospective analysis shows that this new method of Roux-en-Y reconstruction using staplers during PD might reduce the incidence of delayed gastric emptying vs. conventional hand-sewn reconstruction. However, this study is a historical cohort analysis of one surgeon's experience. The improvement in the surgeon's skills, the change in drainage-tube placement, and the early return to a normal diet may have created bias. Thus, further study will be necessary to evaluate the utility of this new method.

Acknowledgment. This work was supported in part by Grant-in-Aid for scientific research from the Ministry of Education, Science and Culture, and the Ministry of Health and Welfare of Japan

References

1. Nomura S, Sasako M, Katai H, Sano T, Maruyama K. Decreasing complication rates with stapled esophagojejunostomy following a learning curve. Gastric Cancer 2000;3:97–101.
2. Hansen O, Schwenk W, Hucke HP, Stoch W. Colorectal stapled anastomoses. Experiences and results. Dis Colon Rectum 1996; 39:30–6.
3. Köckerling F, Rose J, Schneider C, Scheidbach H, Scheuerlein H, Reymond MA, et al. Laparoscopic colorectal anastomosis: risk of postoperative leakage. Results of a multicenter study. Laparoscopic Colorectal Surgery Study Group (LCSSG). Surg Endosc 1999;13:639–44.
4. Tanaka M. Gastroparesis after a pylorus-preserving pancreatoduodenectomy. Surg Today 2005;35:345–50.
5. van Berge Henegouwen MI, van Gulik TM, DeWit LT, Allema JH, Rauws EA, Obertop H, et al. Delayed gastric emptying after standard pancreaticoduodenectomy versus pylorus-preserving pancreaticoduodenectomy: an analysis of 200 consecutive patients. J Am Coll Surg 1997;185:388–95.
6. Park YC, Kim SW, Jang JY, Ahn YJ, Park YH. Factors influencing delayed gastric emptying after pylorus-preserving pancreatoduodenectomy. J Am Coll Surg 2003;196:859–65.
7. Yeo CJ, Barry MK, Sauter PK, Sostre S, Lillemoe KD, Pitt HA, et al. Erythromycin accelerates gastric emptying after pancreaticoduodenectomy. A prospective, randomized, placebo-controlled trial. Ann Surg 1993;218:229–38.
8. Kim DK, Hindenburg AA, Sharma SK, Suk CH, Gress FG, Staszewski H, et al. Is pylorospasm a cause of delayed gastric emptying after pylorus-preserving pancreaticoduodenectomy? Ann Surg Oncol 2005;12:222–7.
9. van Berge Henegouwen MI, Akkermans LM, van Gulik TM, Masclee AA, Moojen TM, Obertop H, et al. Prospective, randomized trial on the effect of cyclic versus continuous enteral nutrition on postoperative gastric function after pylorus-preserving pancreatoduodenectomy. Ann Surg 1997;226:677–87.
10. Tani M, Terasawa H, Kawai M, Ina S, Hirono S, Uchiyama K, et al. Improvement of delayed gastric emptying in pylorus-preserving pancreaticoduodenectomy. Results of a prospective, randomized, controlled trial. Ann Surg 2006;243:316–20.
11. Murakami H, Yasue M. A vertical stomach reconstruction after pylorus-preserving pancreaticoduodenectomy. Am J Surg 2001;181:149–52.
12. Sugiyama M, Abe N, Ueki H, Masaki T, Mori T, Atomi Y. A new reconstruction method for preventing delayed gastric emptying after pylorus-preserving pancreatoduodenectomy. Am J Surg 2004;187:743–6.
13. Tran KT, Smeenk HG, van Eijck CH, Kazemier G, Hop WC, Greve JW, et al. Pylorus preserving pancreaticoduodenectomy versus standard Whipple procedure. A prospective, randomized, multicenter analysis of 170 patients with pancreatic and periampullary tumors. Ann Surg 2004;240:738–45.
14. Shimada K, Sano T, Sakamoto Y, Kosuge T. Clinical implications of combined portal vein resection as a palliative procedure in patients undergoing pancreaticoduodenectomy for pancreatic head carcinoma. Ann Surg Oncol 2006;13:1569–78.
15. Sakamoto Y, Shimada K, Esaki M, Kajiwara T, Sano T, Kosuge T. Wrapping the stump of the gastroduodenal artery using the falciform ligament during pancreaticoduodenectomy. J Am Coll Surg 2007;204:334–6.
16. Bassi C, Dervenis C, Butturini G, Fingerhut A, Yeo C, Izbicki J, et al. Postoperative pancreatic fistula: an international study group (ISGPF) definition. Surgery 2005;138:8–13.
17. Tanaka M, Sarr MG. Role of the duodenum in the control of canine gastrointestinal motility. Gastroenterology 1988;94: 622–9.
18. Ueno T, Tanaka A, Hamanaka Y, Tsurumi M, Suzuki T. A proposal mechanism of early delayed gastric emptying after pylorus preserving pancreatoduodenectomy. Hepatogastroenterology 1995;42:269–74.